SEA GRANT PROGRAM

The Use of Carbon and Sulfur Isotopic Ratios and Total Sulfur Content for Identifying the Origin of Beach Tars in Santa Monica Bay, California

by Blayne Alan Hartman

June 1978

Thesis/Dissertation Series
USCSG-TD-02-78

USC
imcs

THE USE OF CARBON AND SULFUR ISOTOPIC RATIOS AND TOTAL SULFUR CONTENT FOR IDENTIFYING THE ORIGIN OF BEACH TARS IN SANTA MONICA BAY, CALIFORNIA

by

Blayne Alan Hartman

A Thesis Presented to the

FACULTY OF THE GRADUATE SCHOOL

UNIVERSITY OF SOUTHERN CALIFORNIA

In Partial Fulfillment of the

Requirements for the Degree

MASTER OF SCIENCE

(Geological Sciences)

June 1978

CONTENTS

ILLUSTRATIONS

Figure Page

Appendix Figure

TABLES

ABSTRACT

Carbon and sulfur isotopic ratios and total sulfur content are evaluated as chemical fingerprints for highly weathered petroleum in the marine environment. Analysis is confined strictly to the asphaltene fraction of petroleum owing to the insensitivity of the fraction to weathering processes. The technique is applied to the problem of the source identification of tar depositing on the coastline adjacent to metropolitan Los Angeles, California.

The $\delta^{13}C$, $\delta^{34}S$, and %S of the asphaltene fraction of natural offshore seep oils range from -22.51‰ to -23.20‰, +7.75‰ to +15.01‰, and 4.45% to 8.27%, respectively. Values for local offshore production wells overlapped those for the natural seepage, ranging from -22.10‰ to -22.85‰, -2.96‰ to 13.90‰ , and 0.81% to 8.00%. Analytical values for these parameters show that tanker crudes imported into the area are not similar to the California oils.

Comparison of the same parameters from beach tars collected during the 1976-1977 years to the parameters of the potential source oil suggests that 51% of the tars in Santa Monica Bay are derived from natural oil seepage at Coal Oil Point, 31% from natural oil seepage in Santa Monica Bay, and 18% from unknown sources.

The chemical data, coupled with seasonal monitoring of tar deposition and slick size at oil seeps, allow models of tar transport

to be deduced. Tar from the Coal Oil Point natural oil seeps is transported southward in the southern California gyre during the spring, summer, and fall seasons, but undergoes northward transport during the winter season due to the surfacing of the Davidson current. Tar from the Santa Monica Bay natural oil seeps in transported by a circulation pattern consisting of one or more surface current gyres. The ultimate fate of tars depositing in Santa Monica Bay is transport into the Santa Monica Basin and incorporation into the sediment column.

ACKNOWLEDGEMENTS

This project relied on the assistance of so many people that it is impossible for me to personally acknowledge everyone. I express my appreciation to those of you I forget to mention.

Thanks are extended to my fellow students who contributed in the laboratory, Mark Rowley, Brian Wernicke, Sandra Limerick, Gayle Haraguchi, and especially to Jeri Lynn Cameron, for her constant smile. Special mention is given to my diving partners, Sam Limerick and Tom O'Neil, who endured the hardships of the trips to the oil seeps.

Special thanks are extended to the following people: Lt. John McFarlane and the L.A. County lifeguards, who helped with the collection and observation of beach tar, Dr. Robert Sweeney for his positive comments and suggestions throughout the study, Dave Winter, who ran the sulfur samples on the mass spectrometer, Dr. Robert Given for providing facilities at the Catalina Marine Science Station, Glen Ledingham, who tracked down well locations, Dr. Peter Fischer for his comments and the use of his secretary and draftswoman, and to Dr. Ronald Kolpack and Dr. Teh-Lung Ku for their comments and criticisms.

Patti Cournoyer managed to type the complete manuscript and still keep smiling, and Gina VanderGiessen and Debbie Nishida did an excellent job on the drafting of figures.

This report was funded by the Office of Sea Grant, Department of

Commerce under grant #04-6-158-4418 to the University of Southern California.

Finally, my deepest appreciation to two very special people: Dr. Douglas Hammond, who provided assistance and encouragement well beyond the limits of the project and lastly, to Wendy, whose love and patience kept me strong.

INTRODUCTION

General Statement

The result of the depletion of terrestrial petroleum reserves will be an increase in the offshore exploitation of petroleum. This increase in offshore production will increase the potential for pollution of the coastal ocean by petroleum.

At present, the identification of the source(s) of highly weathered petroleums found in the marine environment is not possible. Unless techniques enabling source identification are developed, an increase in the careless and illegal handling of petroleum in the ocean appears evident. The net result will be an increase in the contamination of the coastal margins by oil and tar.

The southern California Borderland offers an ideal location to test characterization procedures. Its coastline has been contaminated by the occurrence of oil and tar deposits for hundreds of years, particularly along the coastline from Point Conception to the Palos Verdes peninsula (Figure 1). The tar deposits represent the residuum from fresh petroleum after extreme exposure to the marine environment.

The purpose of this study was to examine the stable isotopic ratios of carbon and sulfur, and the total sulfur content, in the asphaltene fraction of petroleum and to assess their use as chemical fingerprints for highly weathered marine petroleums. These techniques were then

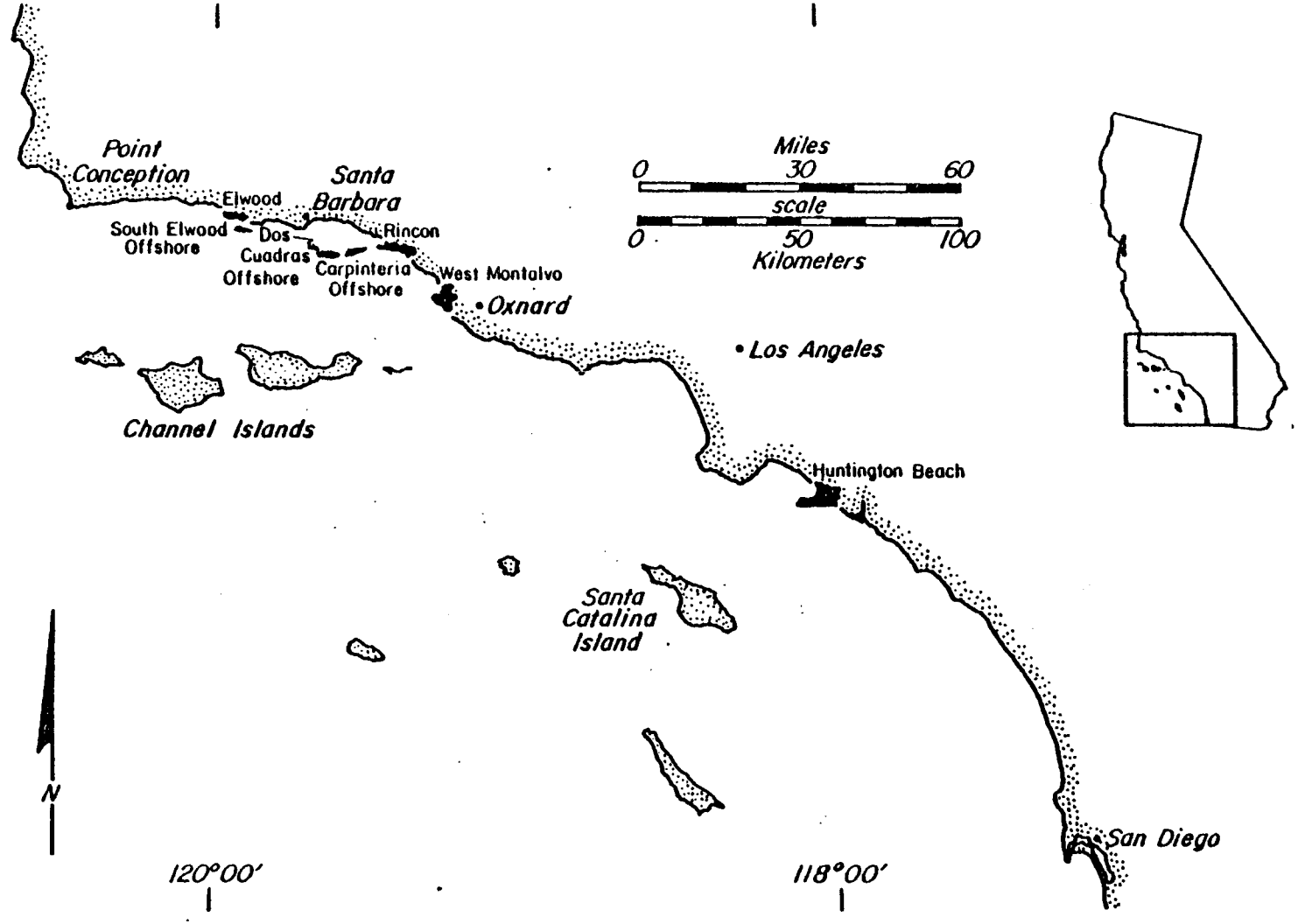

Figure 1. The southern California coastal zone and locations of offshore oil fields sampled during this study.

applied to the problem of identifying the source(s) of beach tars found in Santa Monica Bay, California.

Principles of Fingerprinting

The identification and characterization of petroleum on the basis of its chemical properties is commonly referred to as chemical fingerprinting. A parameter must fulfill two criteria in order to be useful as a fingerprint for marine petroleums: (1) it must exhibit a variation among different petroleums, particularly those petroleums which are produced or transported in the same locale; (2) it must be relatively insensitive to chemical alteration processes upon exposure to the natural environment.

The past ten to fifteen years of research has focused on the search for specific properties of petroleum which fit these criteria. Many techniques, such as gas chromatography, infrared spectroscopy, and trace metal analysis, have been widely used to develop fingerprints, but these methods permit only limited application (Adlard, 1972; Kreider, 1971; Koons et al., 1971).

The stable isotopic ratios of carbon and sulfur have not been investigated in detail, primarily due to the complex and precise laboratory preparation and instrumentation required. On the basis of present models of petroleum evolution, it is probable that these two parameters may exhibit a variation among petroleums. Petroleum is believed to be formed by the degradation of organic material through a series of poorly understood anaerobic reactions. The immature petroleum inherits a carbon isotope ratio ($^{13}C/^{12}C$) similar to the

lipid fraction of the original organic material. This ratio subsequently increases as the petroleum is subjected to maturation processes (Silverman, 1964). The final isotopic ratio of the mature petroleum is characteristic of that reservoir.

Based on this model of evolution, the carbon isotopic ratio is dependent upon: (1) the isotopic ratio of the source material; (2) the degree and extent of reservoir maturation. Generally, petroleums derived from source rocks of different age and location have different carbon isotopic ratios, although this variation may be masked if the maturation histories were quite different.

The process(es) by which sulfur is incorporated into petroleum is also poorly understood. Until the 1970's, it was generally accepted that the majority of sulfur in petroleum was incorporated by the bacterial reduction of seawater sulfate (Thode and Monster, 1970). This mechanism resulted in an enrichment of the lighter sulfur isotope (^{32}S) in the immature petroleum. The sulfur isotopic ratio ($^{34}S/^{32}S$) was believed to be 15-20‰ lower in the petroleum relative to seawater sulfate and to be insensitive to maturation processes.

More recently, Vredenberg and Cheney (1971) postulated that this ratio had been altered in petroleums from the Wind River Basin. Orr (1974), basing his conclusion on values from oils from the Big Horn Basin, suggested that petroleum may lose or gain significant quantities of sulfur through kinetically controlled sulfurization and desulfurization processes. Thus, the sulfur isotope ratio tends to approach the value of the reservoir water sulfate which in this case is controlled by

nearby evaporite deposits in the basin. Sweeney (1977) using the ratio of sulfur to nitrogen and $\delta^{34}S$ predicts distinct episodes of sulfurization and desulfurization for California oils; the history of which could be significantly different from Big Horn Basin oils due to the lack of evaporites in the California basins.

In summary, the sulfur isotopic ratio for a given petroleum depends upon: (1) the $^{34}S/^{32}S$ ratio of the sulfur initially incorporated in the petroleum; (2) the $^{34}S/^{32}S$ ratio of the formation water sulfate; (3) the degree of sulfurization and desulfurization processes during maturation.

Although petroleums from different reservoirs may frequently exhibit similar carbon or similar sulfur isotopic ratios, the number of petroleums having both ratios identical should be low based on the large number of evolutionary variables involved.

Weathering

The chemical characterization of crude oil is routinely performed by a large number of laboratories using a variety of parameters. Once the petroleum has been exposed to the marine environment, the task is no longer routine. Complications are introduced after the petroleum compounds are subjected to chemical, physical, and biological processes that are operative during exposure in the natural environment.

Weathering of petroleum in the marine environment has been intensively studied (Brunnock et al., 1968; Blumer and Sass, 1972; Ehrhardt and Blumer, 1972; Koons, 1972) and reviewed (Kolpack et al., 1973; National Academy of Sciences, 1975). Four processes are generally responsible for the majority of petroleum weathering: (1) evaporation

of the volatile components; (2) dissolution into the water column; (3) photooxidation; (4) biodegradation.

The lighter components of petroleum are highly susceptible to weathering reactions. For example, Kinney et al. (1969), Smith and MacIntyre (1971), and Kreider (1971) conducted various simulation and field studies on petroleum weathering and concluded that after 24 hours of exposure to the marine environment, less than ten percent of the low molecular weight components were still present in the residuum (Figure 2).

The rate of weathering varies, depending primarily upon temperature, film thickness, turbulence, and solar intensity (National Academy of Sciences, 1975). After extreme weathering, generally for exposure times of one month or greater, the chemistry of the residuum is unlike the original petroleum as it consists primarily of high molecular weight compounds. The initial petroleum slick typically fragments into patches of thick oil (Jeffrey, 1973), which eventually become hard masses of tar. These tars may then be transported shoreward or owing to increased density, sink to the bottom.

At present, chemical procedures that are used in an attempt to trace highly weathered oils and tars to their source utilize the entire range of petroleum compounds. It most cases, however, the chemistry of the weathered petroleum no longer resembles the chemistry of the original petroleum, introducing considerable doubt into the identification. The heavier fractions of petroleum, such as the resins and asphaltene compounds are not lost or modified as rapidly as a result of weathering

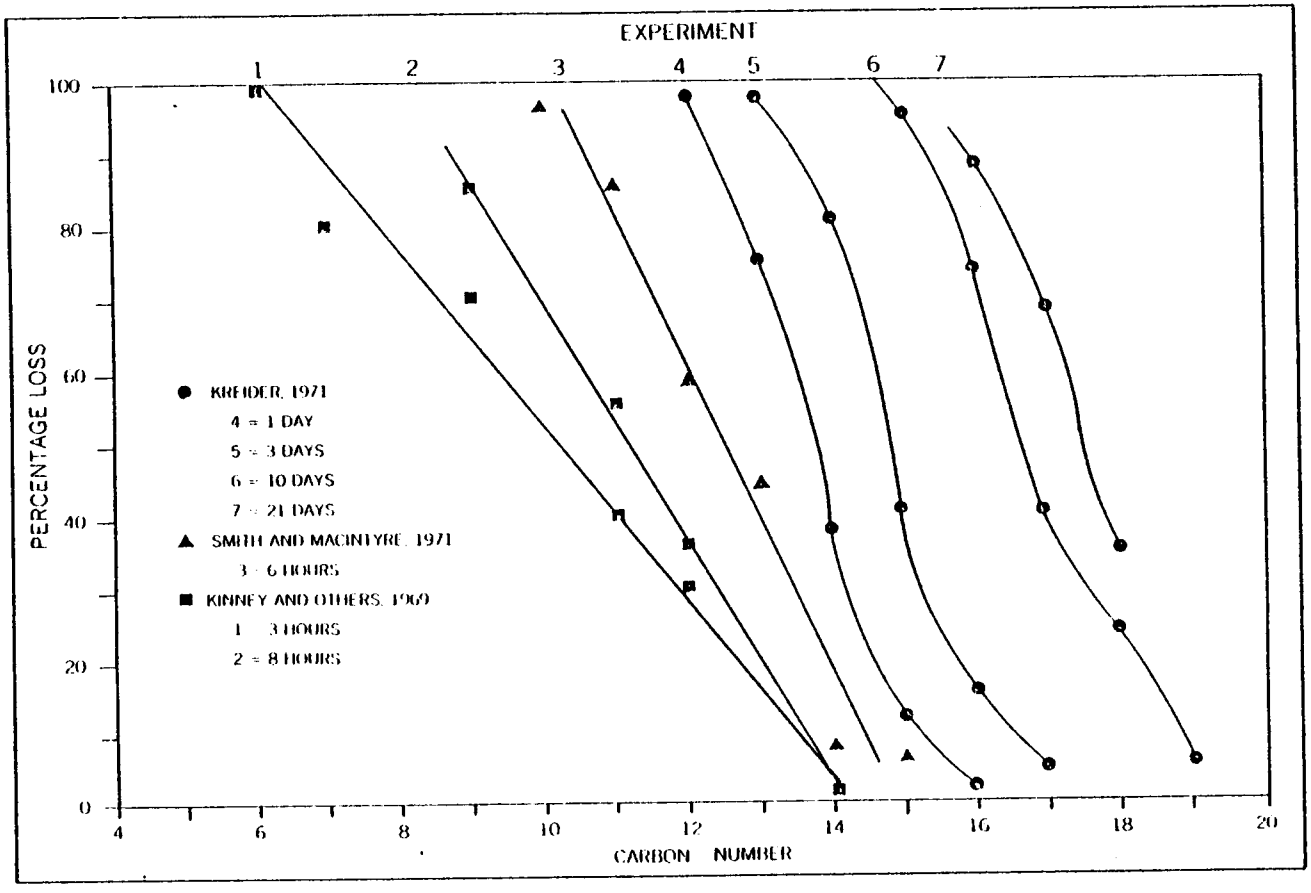

Figure 2. Summary of percentages of evaporative losses from two crude oils (Kreider, 1971 and Kinney et al., 1969) and a #2 fuel oil (Smith and MacIntyre, 1971) (after Kolpack et al., 1973).

(Blumer et al., 1973). Consequently, the chemical characterization of these fractions may prove useful to identify the sources of highly weathered petroleums.

The asphaltic fraction of petroleum consists of a complex aggregate of a large number of compounds, existing as colloidal particles (Witherspoon and Winniford, 1967). This fraction is loosely defined as the bottoms after non-destructive distillation at 371°C (ASTM D86-61).

The asphaltenes are defined as the pentane insolubles in the asphaltic fraction. A variety of procedures have been developed to separate the asphaltenes from petroleum; a comprehensive summary is given by Witherspoon and Winniford (1967).

The molecular weights of the asphaltenes have not been firmly established. A large number of methods have been employed in the determination of molecular weight, yielding a large range of values. An average range may be taken as 1,000-10,000, suggesting a significant amount of heterogeneity in this fraction.

Structural investigations of the asphaltenes indicate an aromatic character. Yen (1974) concluded that the asphaltene structure consists of polynuclear aromatic ring systems, containing as many as twenty fused rings. Combustion analyses have shown that this fraction can contain large amounts of NSO compounds within its structure.

Although the asphaltene fraction is relatively insensitive to weathering reactions, it has been suggested (Betancourt and McLean, 1973) that asphaltenes may be formed by the photooxidation of petrolenes during long exposure to the marine enviornment. O'Neil (1978)

conducted laboratory simulations on the formation of asphaltenes, using de-asphaltened oils. He concluded that the increase of asphaltenes after 100 days of simulated weathering was a maximum of 1% of the original quantity of asphaltenes.

The change in the value of a chemical parameter in the asphaltene fraction due to this formation may be represented as:

$$\Delta Y_a = ((1-x)Y_o + xY_i) - Y_o$$

Where: ΔY_a represents the change of any paramter, Y;

x fraction of asphaltenes formed;

o asphaltene fraction before growth;

i petrolene fraction before growth.

For the isotopic ratio in the asphaltene fraction, this expression becomes:

$$\Delta\delta A = ((1-x)\delta A_o + x\delta_i) - \delta A_o$$

Expanding:

$$\Delta\delta A = \delta A_o - \delta A_o + x\delta A_0 - x\delta_i$$

Simplifying:

$$\Delta\delta A = x(\delta A_o - \delta i)$$

And:

$$x = \Delta\delta A/ (\delta A_o - \delta_i)$$

Silverman and Epstein (1958) measured the $\delta^{13}C$ in the various fractions of petroleum and observed a range of 1.1‰, from -22.3‰ to -23.4‰. Monster (1972) examined the ranges of the isotopic ratios of both carbon and sulfur in three Saskatchewan oils and observed an average maximum heterogeneity between petroleum fractions of 0.81‰ and

1.5‰, respectively. Most recently, Reed and Kaplan (1977) reported a maximum range of 2.42‰ for the carbon isotope ratio in the fractions of four California seep oils, although they did not separate the asphaltenes from the petrolenes.

Based on these studies, conservative estimates for the deviation of $\delta^{13}C$ and $\delta^{34}S$ between asphaltenes and petrolenes may be taken as 1‰ and 1.5‰, respectively. Assuming an analytical precision of 0.10‰ and 0.30‰ for $\delta^{13}C$ and $\delta^{34}S$, the quantity of formed asphaltenes required to cause a significant error may be calculated as:

$$\delta^{13}C: \quad x = \frac{\delta A}{\delta A_o + \delta_i} = \frac{0.1‰}{1‰} (100\%) = 10\%$$

$$\delta^{34}S: \quad x = \frac{0.3‰}{1.5‰} (100\%) = 20\%$$

These calculations indicate that at least a 10% increase of asphaltenes from petrolenes is required to introduce significant error into the measured isotopic ratios. This result is an order of magnitude greater than the amount formed in O'Neil's (1978) weathering study.

Study Location

There are three potential sources of large petroleum inputs into the southern California coastal waters: (1) natural oil seepage; (2) production of offshore oil; (3) handling and transport of locally produced crudes and imported crudes.

The natural leakage of oil out of cracks and fissures in the crust is known as a natural oil seep. Southern California, owing to its oil rich strata and complex structure has been classified as a region of very high seep potential (Wilson et al., 1973). Wilkinson (1971) has

documented over 50 areas of offshore oil and gas seepage off the southern California coast. Despite the large number of seepage areas, only two locations contribute a significant amount of oil to the coastal waters.

The Coal Oil Point seepage, located approximately 30 kilometers west of Santa Barbara, originates from the offshore extension of the oil rich Ventura Basin (Figure 3). This seepage area consists of a number of active seepage vents, ranging in water depth from 10 to 100 meters, which are commonly grouped into zones of heavy seepage. Wilkinson (1971) distinguishes three zones of active seepage, the Coal Oil Point, Isla Vista, and La Goleta seepage zones (Figure 3). Fischer and Berry (1973) correlate zones of active seepage to submarine structure and identify six major seepage zones (Figure 3). However, their classification differs from the one used by Wilkinson (1971). Estimated rates of petroleum seepage from this area range from 50 to 70 barrels per day (Mikolaj et al., 1972) to 900 barrels per day (Straughan and Abbott, 1971). In addition, despite the abundant chemical, geological, and physical data collected from this seepage area, controversy still exists over the source rocks of the seeping petroleum.

There are two areas of natural seepage in Santa Monica Bay, the Redondo Canyon seep and the Manhattan seep (Figure 4). The Redondo Canyon seep is generally believed to occur along the Palos Verdes fault in the nearshore portion of the Redondo submarine canyon.

The exact location of the seepage is not known due to the large

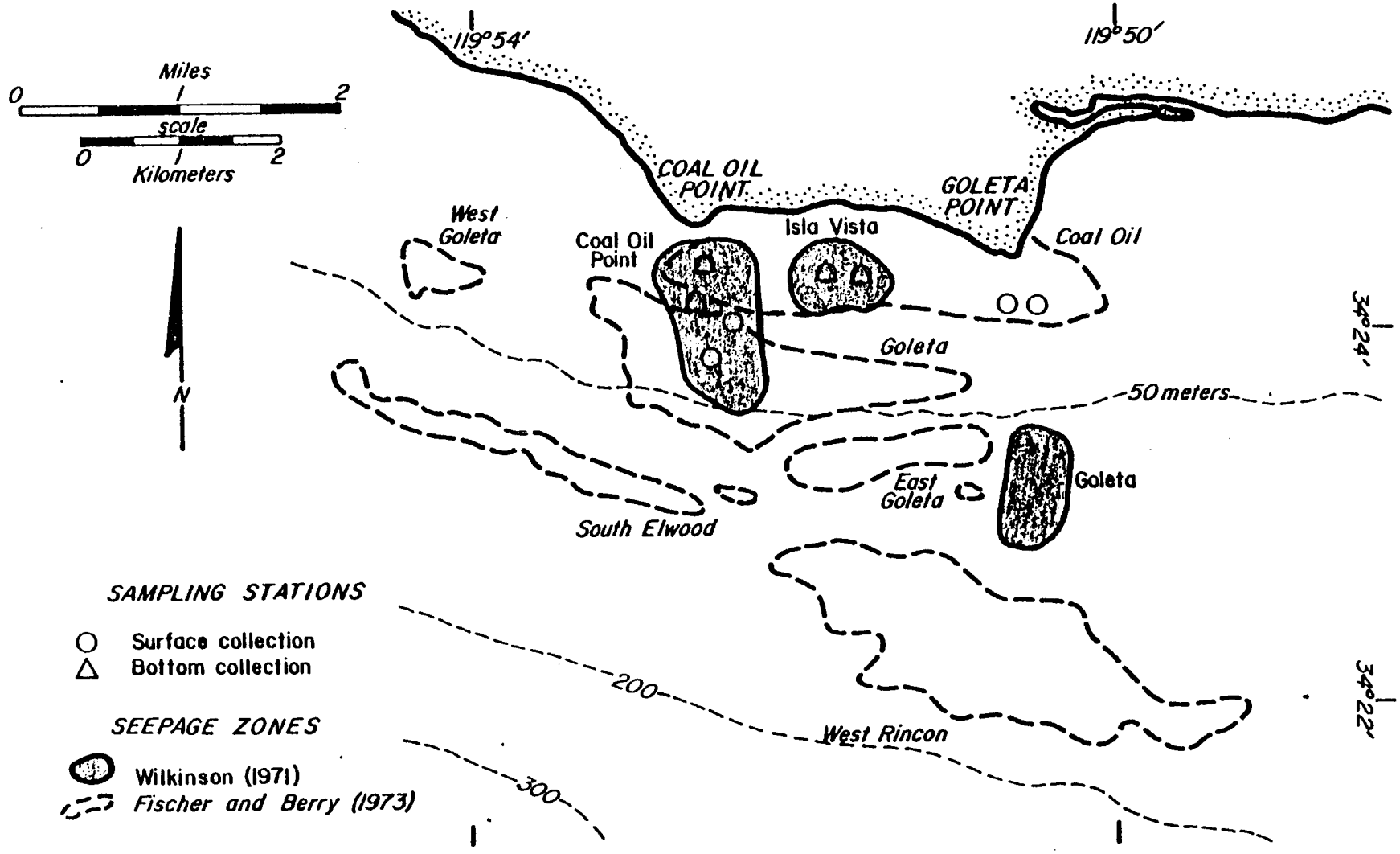

Figure 3. Natural oil seepage zones and sampling stations at Coal Oil Point (after Fischer and Berry, 1973).

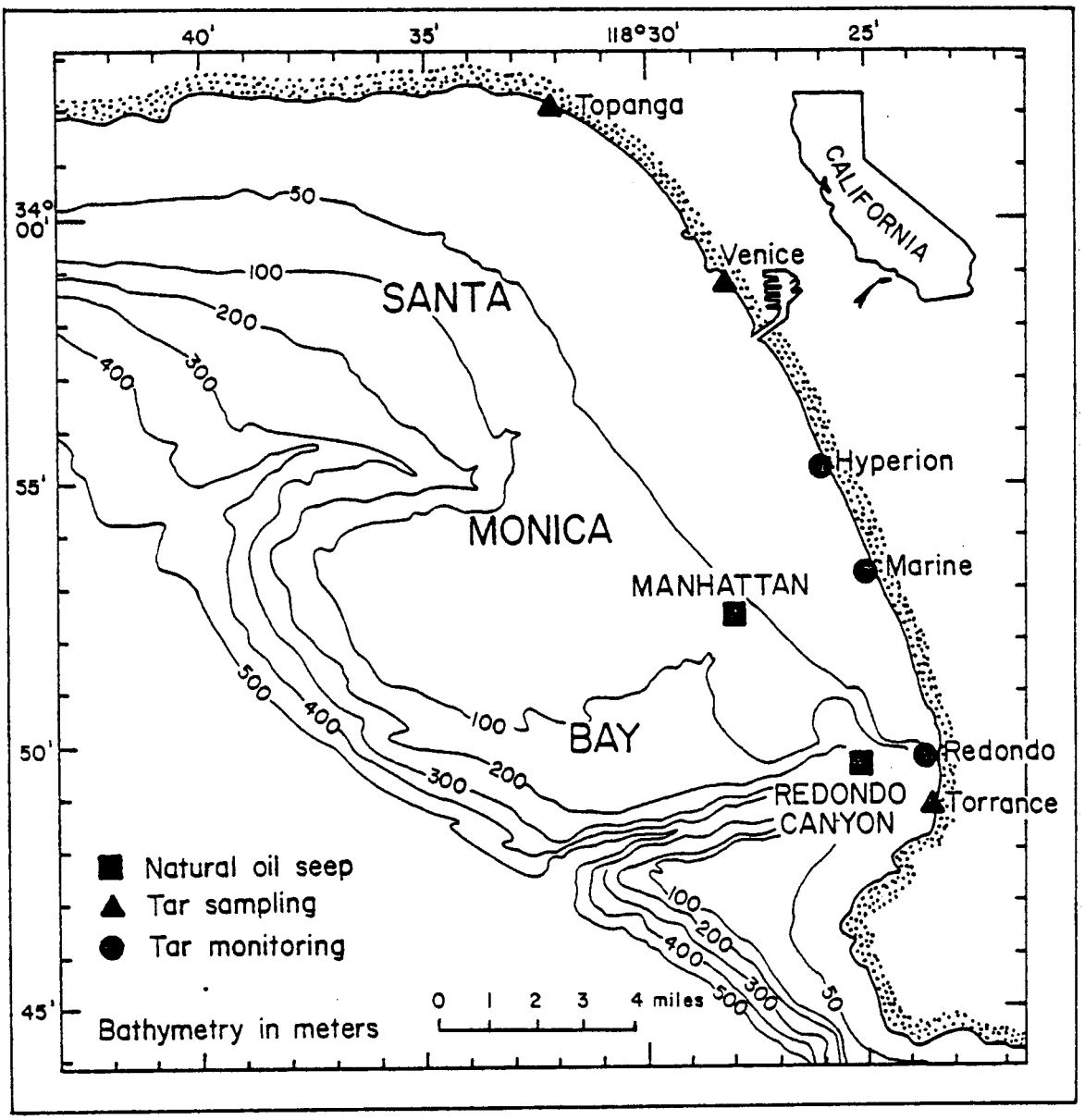

Figure 4. Bathymetry of Santa Monica Bay and locations of natural seepage zones and sampling stations.

water depth which has prohibited detailed investigation by SCUBA. Visual observation of surface slicks, however, suggests that petroleum is escaping from two or possibly three different locations in the canyon. The Manhattan seepage is located farther offshore than the Redondo Canyon seep, as deduced from slick location. This seep is also believed to originate along the Palos Verdes fault, although the source rocks for both seepage zones are unknown (Wilkinson, 1971).

The combined seepage rate of petroleum from these seeps is estimated to be 10-12 barrels/day (Mikolaj et al., 1972) and 10-15 barrels/day (Wilkinson, 1971). Although these combined seepage rates are nearly an order of magnitude less than the rate at Coal Oil Point, these seeps have received widespread attention owing to their close proximity to metropolitan Los Angeles.

The amount of petroleum that enters the southern California coastal waters from man-induced sources, such as offshore production and tanker transport, is more difficult to determine. Occasionally, large quantities of oil are injected into the ocean by a major mishap, such as the 1969 Union Oil Company Platform A blowout; however, large inputs are quickly detected and easily traced to source.

Less conspicuous are the small inputs of oil from these sources due to daily operations such as the disposal of drilling muds and flushing of ballast tanks. Although the potential input of petroleum from these sources is high due to the numerous production platforms and frequent tanker traffic through the Santa Barbara Channel, it is difficult to estimate how much of the tar found on beaches they may contribute.

Previous Work

Numerous studies (Allen and Schlueter, 1969; Chapin, 1972; Delaney, 1972; Mikolaj et al., 1972) have concentrated on the tars depositing along the southern California coastline, particularly along the shoreline extending from Point Conception to Santa Barbara. A comprehensive review of this literature is described by O'Neil (1978).

Only three previous studies have concentrated on tars found along the coast of Santa Monica Bay. Ludwig and Carter (1961) attempted to characterize beach tar on the basis of its chemical and physical properties, such as size, appearance and percent solubles in various organic solvents. Chemical properties of the tars were determined using methods developed by Merz (1959). Their conclusions were that the tars washing ashore appeared to be similar to petroleum from natural oil seeps. They did not conclude from which seep the tars originated (Table 1).

Allen et al. (1971) conducted a similar investigation for the Standard Oil Company. The project was intended to study the effect of the offshore unloading of petroleum to the company's El Segundo refinery on the surrounding coastline. Basing their identification predominately on gas chromatography and to a lesser extent on the ratio of nickel to vanadium, they concluded that 86% of the tar deposits in Santa Monica Bay originated from the natural oil seepages in Santa Monica Bay (Table 1). The authors accounted for weathering effects by assuming a constant weathering loss of fifteen percent.

More recently, O'Neil (1978) investigated the asphaltene fraction of beach tars and marine oils in an attempt to minimize errors introduced by weathering processes. O'Neil, basing his conclusions on the

Table 1. Results of previous studies on characterization of tars in Santa Monica Bay.

Study	Tar Origin (%)			Comments
	Natural Seepage		Unknown	
	Coal Oil Point	S. M. Bay		
Ludwig & Carter (1961)	100			Could not distinguish between seeps. Used total oil.
Allen et al. (1971)	0	86	14	Based primarily on gas chromatography of total oil. Weathering correction.
O'Neil (1978)	30	56	14	Based on Ni, V, & S in asphaltene fraction.

total content of nickel, vanadium, and sulfur, deduced that 56% of the tars found in Santa Monica Bay originated from the seeps in Santa Monica Bay and 30% from seepage at Coal Oil Point (Table 1). Although all three studies conclude that the majority of the tars found in Santa Monica Bay are derived from natural oil seepage, there is disagreement as to the fraction contributed by each seep. Clearly, there is a need to resolve this conflict of opinion if efforts to stop beach contamination are to be successful.

METHODS

Sampling Techniques

Samples were collected from each of the major potential sources of petroleum in the southern California coastal zone. These sources included samples from the areas of natural oil seepage, offshore production platforms, and tanker crudes off-loaded in Santa Monica Bay.

Samples from the natural oil seeps were collected on eight different dates from September, 1976 to June, 1977. These samples included 20 aliquots from the three major seepage zones at Coal Oil Point (Figure 3) and five aliquots from the two major seepage zones in Santa Monica Bay (Figure 4). Samples were collected from the sea bottom by SCUBA divers and from the water surface when SCUBA collection was not possible.

Asphaltene samples from 10 crude oils produced in the southern California coastal zone (Figure 1) were obtained from Thomas O'Neil. Aliquots of the major imported foreign crudes to the El Segundo refinery were obtained from the Standard Oil Company of California.

Tar lumps were collected twice per month for a full calendar year at three beaches in Santa Monica Bay (Figure 4). In addition, tars were collected less frequently from beaches located northwest and southeast of Santa Monica Bay. Three individual lumps, varying in length from 3 to 30 cm, were collected on each sampling day to enable the identification of tar from multiple sources reaching the beach on the same day.

A fourth tar sample, consisting of an aggregate of large (>3 cm) and small (< 3 cm) lumps, was collected at random. This sample was homogenized and the analytical results were compared to the individual tar lumps to test the possibility that different sized lumps have different sources.

Collected samples were stored immediately in sealed glass containers. Poisoning of samples with mercuric chloride to reduce biological degradation during storage was found to be unnecessary by analytical comparison of poisoned and unpoisoned aliquots of the same sample.

Laboratory Procedures

Samples were cleaned of large organic and foreign debris and separated from entrapped sand by soxhlet extraction with toluene. The asphaltene components were separated by precipitation in 20 volumes of pentane and purified by washing with pentane. The precipitate was redissolved in toluene and freeze-dried, yielding a brown to black powder.

Small aliquots of asphaltene (7 mg) were combusted at 900°C and 700 mm of oxygen over CuO catalyst for the preparation of carbon dioxide gas to be used for isotope analysis (Kaplan et al., 1970). The CO_2 gas was collected, sealed in glass tubes, and analyzed on a dual collector, Nuclide mass spectrometer.

Total sulfur content was determined gravimetrically by combustion of 0.5 g of asphaltene in 30 atmospheres of oxygen and subsequent precipitation as $BaSO_4$ (Parr Instrument Company, 1964). Analytical precision was $\pm$5.0% of the measurement. Sulfur dioxide was prepared for

isotopic analysis by combustion of 20 mg of $BaSO_4$ in the presence of heated metallic copper (Bailey and Smith, 1972). The SO_2 was analyzed on a dual collector Nuclide mass spectrometer by David Winter at the University of California, Los Angeles.

Isotopic data for both carbon and sulfur are expressed relative to Chicago PDB carbonate and Canyon Diablo trolite respectively, in the conventional δ notation:

$$\delta X_{\text{sample}} ‰ = \frac{Y \text{ sample} - Y \text{ standard}}{Y \text{ standard}} \times 1000$$

Where X represents the element of interest and Y the ratio of rare to the most abundant isotope of that element. The reported sulfur isotopic ratios are uncorrected for the $\delta^{18}O$ of the tank oxygen used in the formation of the barium sulfate precipitate. This correction does not affect the relative variation in sulfur isotopic ratio between the analyzed samples. Analytical precision of the reported values is $\pm$0.08‰ and $\pm$0.35‰ for carbon isotopes and sulfur isotopes, respectively.

Detailed descriptions of the analytical procedures, ultra-high vacuum extraction systems, and equipment calibrations are summarized in the appendix.

Weathering Experiments

The relative insensitivity of the asphaltene fraction of petroleum to weathering processes was tested by two methods, a controlled weathering simulation experiment and a beach weathering experiment.

The controlled weathering experiment consisted of three plexi-glass tanks, 120 x 76 x 45 cm, filled with seawater (See Appendix). A continuous flow system fed seawater to the tanks at a rate of approximately

300 ml/min, flushing the tank an average of three times per day. Tanks were set outdoors at the University of Southern California Catalina Island marine science facility where solar radiation and wind convection would simulate natural conditions as closely as possible.

Three types of petroleums were weathered, a low sulfur crude imported from Sumatra, a local offshore produced crude, and a natural seep oil from Coal Oil Point. Samples (25 g) were taken after 33, 50, and 100 days of exposure and analyzed for total sulfur content and isotopic ratios as previously described. The degree of weathering was monitored by periodic gas chromatographic analyses of the residuum.

The beach weathering experiment consisted of the collection of tars from a beach with tar concentrations exceeding 500 g/m of beachfront. The rocky headland at Coal Oil Point was chosen as the best location for this study as its close proximity to the Coal Oil Point natural seepage insured that all tars were derived from the same source. Tars were selected on the basis of the degree of weathering by natural elements, as estimated by the physical appearance of the lumps. Three types of tars were collected: (1) fresh tar: soft, pliable tar smelling strongly of petroleum and containing little sand; (2) weathered tar: hard, pliable tar with a slight petroleum smell and containing abundant sand; (3) highly weathered tar: hard, brittle tar with no odor and firmly encased in sand. This tar was typically denser than seawater.

Samples of oil from the controlled weathering experiment were dissolved in small volumes of xylene (1:3) and stored in sealed glass tubes for chromatographic analysis. Five microliter aliquots of each sample were injected into a temperature programmable Chromalytics MP-3

gas chromatograph equipped with a flame ionization detector and packed with 2m x .32cm column of OV101 (80/100 mesh). Column temperature was increased at 8°/min from 50°C to 280°C. Peak positions were determined by injection of a mixed alkane standard in xylene.

Monitoring of Tar Deposition and Natural Oil Seepage

A monitoring program, designed to correlate patterns of tar deposition with the chemical data, was established with the assistance of the Los Angeles Department of Beaches and the U.S. Coast Guard.

Visual surveys of the amount of tar washing ashore were performed daily by lifeguards at the three sampling stations in Santa Monica Bay (Figure 4). Lifeguards estimated tar concentration based upon the following scale:

Heavy: frequent tar lumps, spaced approximately 1/2 meter or less apart. Tar concentrations exceeding 500 g/m of beachfront.

Moderate: tar lumps spaced approximately 1 to 5 meters apart. Tar concentrations exceeding 100 g/m of beachfront, 500 g/m.

Low: scattered tar lumps, spaced approximately 5 or more meters apart. Tar concentrations less than 100 g/m of beachfront.

Sightings were taken in the intertidal zone over a minimum of 100 meters of beachfront. In addition, the County released similar records for 1975 and 1977 at three different locations in the bay (Figure 4).

Slick size from the natural oil seepages at Coal Oil Point and Santa Monica Bay are routinely checked on a weekly basis by the U.S. Coast Guard, using visual aerial reconnaissance. These records, for the 1976 and 1977 calendar years, were made available for correlation with beach tar data.

RESULTS

The values of $\delta^{13}C$, $\delta^{34}S$, and %S in the asphaltene fraction from over 90 southern California crude and seep oils and Santa Monica Bay beach tars are listed in Table 2. The range in values for the different oils is shown schematically in Figure 5.

Oils from the natural seeps exhibit a relatively narrow range of $\delta^{13}C$ values, -22.51‰ to -23.17‰. The oil from the Santa Monica Bay seepage zones is enriched in the heavier isotope, -22.51‰ to -22.70‰, relative to the oil from the Coal Oil Point seepage zones, -22.86‰ to -23.17‰. Local offshore produced crudes have a larger range of values than the seep oils, -22.10‰ to -22.85‰, but overlap only the range in values of the oil from the Santa Monica Bay seepage. Foreign crudes imported into Santa Monica Bay from Arabia and Sumatra are depleted in the heavier isotope relative to local oils, -25.60‰ to -25.85‰.

The natural seep oils have high concentrations of sulfur in the asphaltene fraction, ranging from 4.4% to 8.3%. Coal Oil Point seep oil has a higher sulfur content, 7.5% to 8.3%, than oil from the Santa Monica Bay seeps, 4.4% to 6.7%. Petroleums produced offshore exhibit a wide range in this parameter, 0.80% to 8.0%, which encompasses both the ranges in sulfur content for the different seep areas. The two foreign crudes are low in sulfur content, 0.20% to 0.25%.

Sulfur isotope data exhibit trends similar to the trends of the

Table 2. Carbon isotope ratio (as $\delta^{13}C$), total sulfur content, and sulfur isotope ratio (as $\delta^{34}S$) in the asphaltene fraction of potential source petroleums and beach tars occuring in Santa Monica Bay.

Sample	Location	$\delta^{13}C$(‰)	%S	$\delta^{34}S$(‰)	Comments
Natural Seeps					
Coal Oil Point	34°23'40"N 119°51 40 W				
9-17-76 1a		-22.86	7.67	+14.59	Coal Oil Point - tar mound
9-17-76 1b		-22.85	7.98	--	Coal Oil Point - tar mound
9-17-76 1f		-22.94	7.41	--	Coal Oil Point - bottom sample
9-17-76 2a		-23.06	7.49	+14.15	Isla Vista - surface skim
9-17-76 2b		-23.12	7.84	+13.89	Isla Vista - surface skim
9-18-76 2a		-22.96	7.54	--	Isla Vista - surface skim
9-18-76 2b		-22.93	7.72	+13.79	Isla Vista - bottom sample
9-18-76 2c		-23.17	7.94	+14.90	Isla Vista - surface skim
9-18-76 2d		-23.00	7.57	+14.43	Isla Vista - tar mound
10-16-76 1d			7.99	+14.72	Coal Oil Point - surface skim
10-16-76 3a		-22.79	8.27	+12.64	La Goleta - surface skim
10-16-76 3b		-22.82	8.18	+13.82	La Goleta - surface skim
11-15-76 1a		-22.97	7.71	+15.01	Coal Oil Point - tar mound
11-16-76 1c			7.75	--	Coal Oil Point - surface skim
2-03-77 1a		-23.10	7.67	+14.60	Coal Oil Point - bottom sample
2-03-77 1c		-23.00	7.48	+13.71	Coal Oil Point - surface skim
2-11-77 1a		-23.03	7.98	+14.16	Coal Oil Point - bottom sample
Santa Monica Bay	33°49'00"N 118°26 10 W				
11-05-76 5a		-22.70	6.30	+12.20	Redondo - skim (surface)
11-05-76 5b		-22.51	6.45	+12.33	Redondo - skim (surface)
11-05-76 5c		-22.61	6.72	+ 9.85	Redondo - skim (surface)

Table 2. (Con't).

Sample	Location	$\delta^{13}C$(‰)	%S	$\delta^{34}S$(‰)	Comments
6-09-77 5a		-22.57	4.45	+ 7.85	Redondo - skim (surface)
6-09-77 6a		-22.61	4.99	+ 7.70	Manhattan - skim (surface)
Offshore Oil Fields					
Dos Cuadras (Hillhouse)		-22.74	8.00	+13.92	Monterey (Mid-Miocene)
South Elwood		-22.80	7.01	+13.90	Monterey (Mid-Miocene)
Elwood		-23.19	0.81	-02.96	Vaqueros (Lower-Miocene)
Huntington Beach J-50		-22.13	1.00	+10.41	Puente (Upper-Miocene)
Carpinteria		-22.85	3.50	+ 9.46	Pico (Upper-Pliocene)
Carpinteria 012		-22.57	4.06	+ 4.55	Pico (Upper-Pliocene)
Rincon PRC 145.1			2.94	+ 8.75	Pico (Upper-Pliocene)
Rincon 145#6			3.22	+ 7.58	Pico (Upper-Pliocene)
West Montalvo			6.31	+11.25	Sespe (Oligocene)
Dos Cuadras (A)		-22.51	2.59	+ 3.96	Pico (Upper-Pliocene)
Huntington Beach PRC 426-4104			1.70	+ 7.19	Puente (Upper-Miocene)
Tanker Crudes					
Sumatra 116048		-25.60	0.19	+ 4.60	El Segundo Refinery
Arabia 117328		-25.85	0.20	+ 3.75	El Segundo Refinery
Beach Tars					
Torrance	33°48'45"N 118°23 36 W				
9-04-76 1a		-23.32	8.38	--	

Table 2. (Con't.)

Sample	Location	$\delta^{13}C$(‰)	%S	$\delta^{34}S$(‰)	Comments
9-04-76 1b		-22.83	7.82	+14.97	
9-04-76 1b-2		-22.85	7.40	+14.70	
9-04-76 1c		-23.25	8.75	+16.12	
9-04-76 1d		-23.11	8.98	+16.40	
9-20-76 1a		-25.67	3.50	+ 6.02	Hard lump
9-20-76 1b		-23.29	7.57	+15.41	
9-20-76 1c		-26.33	0.42	+ 9.98	
10-07-76 1b		-22.82	0.44	+ 4.86	
1-13-77 1a			8.63	--	
1-13-77 1c			7.23	+12.39	
2-20-77 1a			7.03	+10.27	
3-04-77 1a			6.80	--	
4-09-77 1a		-22.69	7.28	+ 9.71	
4-09-77 1b		-22.98	8.60	+15.67	
4-09-77 1c		-22.70	6.71	+11.96	
4-09-77 1d		-23.06	8.79	+15.85	
5-07-77 1a			7.02	--	
5-07-77 1d			8.75	+14.75	
6-23-77 1a			7.44	+12.24	
Venice Beach	33°58'30"N 118°28 48 W				
8-26-76 10b		-22.91	6.44	+11.60	
8-26-76 10d		-23.03	7.10	+ 8.71	
8-26-76 10e			7.43	+10.92	
8-26-76 10f			5.83	--	
9-14-76 10a			1.90	--	

Table 2. (Con't.)

Sample	Location	$\delta^{13}C$ (‰)	%S	$\delta^{34}S$ (‰)	Comments
9-20-76 10a		-25.85	2.60	+ 6.79	Hard lump
9-20-76 10b		-26.07	2.50	--	Hard lump
9-20-76 10c		-24.02	5.46	--	Hard lump
10-01-76 10b		-23.51	8.04	+15.85	
10-01-76 10c		-26.25	3.20	+ 7.17	Hard lump
10-01-76 10d		-23.30	6.19	+10.23	
10-21-76 10c		-22.79	7.66	--	
11-22-76 10a		-23.11	6.73	+10.80	
11-22-76 10d		-23.47	8.28	+14.89	
12-04-76 10a			6.63	--	
12-04-76 10b			7.11	--	
1-07-76 10b			7.36	--	
2-19-77 10a		-22.77	6.15	--	
2-19-77 10b		-22.65	6.11	+11.22	
3-15-77 10a		-23.09	7.22	+15.51	
3-21-77 10a		-22.80	7.38	+14.21	
3-24-77 10d		-23.12	8.39	+15.76	
4-17-77 10a		-22.79	7.58	+12.87	
4-17-77 10b		-22.88	7.74	+13.18	
5-06-77 10c		-22.89	7.27	+13.39	
5-06-77 10b		-22.98	7.03	+13.82	
6-11-77 10b			7.34	--	
6-11-77 10c			4.20	+ 1.89	Tar sand
7-07-77 10a			6.94	+15.96	
7-11-77 10a			8.93	--	
7-20-77 10a			7.17	+ 9.68	

Table 2. (Con't.)

Sample	Location	$\delta^{13}C$ (‰)	%S	$\delta^{34}S$ (‰)	Comments
Topanga Beach	34°02'30"N 118°32 40 W				
9-17-76 20a		-23.02	8.25	+12.93	
2-18-77 20a			7.21	--	
3-25-77 20a			7.13	+14.75	
3-25-77 20c			7.06	--	
4-06-77 20a			8.05	--	
Seal Beach 30b	33°23'40"N 118°07 35 W	-22.85	7.85	+11.55	South of S.M. Bay
Goleta Beach	34°24'20"N 119°50 43 W		8.13	+14.00	North of S.M. Bay
Blacks Beach	32°40'02"N 117°17 30 W	-23.73	2.15	+ 4.88	Possible tanker spill
Morro Bay	35°20'16"N 120°52 08 W		8.04	--	Collected 1-7-78

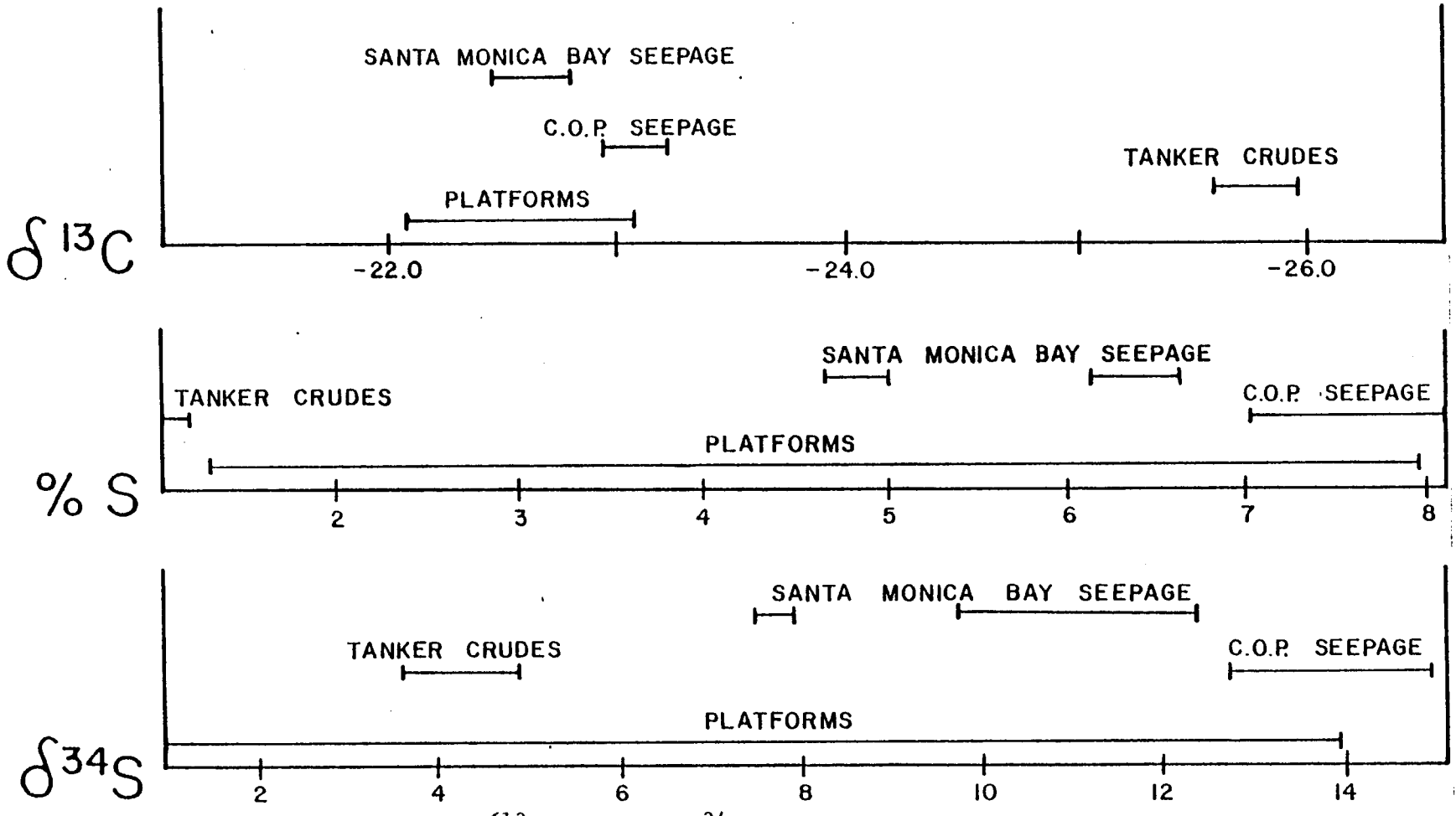

Figure 5. Variation of $\delta^{13}C$, %S, and $\delta^{34}S$ in the asphaltene fraction of potential source oils in the southern California Borderland.

sulfur content data. Seep oils have a highly positive $\delta^{34}S$ value. The Coal Oil Point seep oil is enriched in the heavier isotope, +12.92‰ to +15.01‰, relative to the Santa Monica Bay seeps, +7.70‰ to +12.22‰. Offshore production crudes again exhibit a large range in values, -2.96‰ to +13.92‰, which overlaps the range of the two foreign crudes, +3.75‰ to +4.60‰ and the oil from the Santa Monica Bay seepage.

The differentiation of the oils on the basis of these values is illustrated in Figures 6 and 7. The natural seep oils can be distinguished from all but two of the locally offshore produced crudes and from both of the foreign crudes. In addition, the two areas of natural seepage can be differentiated.

The oils analyzed from the three zones of seepage at Coal Oil Point (Figure 3) are relatively homogeneous for the three parameters investigated, allowing the three individual zones to be referred to collectively as the Coal Oil Point seep. This seep oil is similar, based on the three parameters investigated, to crude oil produced nearby from the Monterey Shale, suggesting Middle Miocene age for the source beds of the seep oil; which is consistent with the result obtained by Reed and Kaplan (1977).

The oils analyzed from the two Santa Monica Bay seepage zones also have uniform $\delta^{13}C$, $\delta^{34}S$, and %S values, but exhibit a variation in chemistry between the two collection dates of November, 1976 and June, 1977. A similar variation was noted by Allen et al. (1971) in the content of nickel and vanadium in the total oil. The oil from these seeps resembles crude produced from the West Montalvo oil field (Sespe

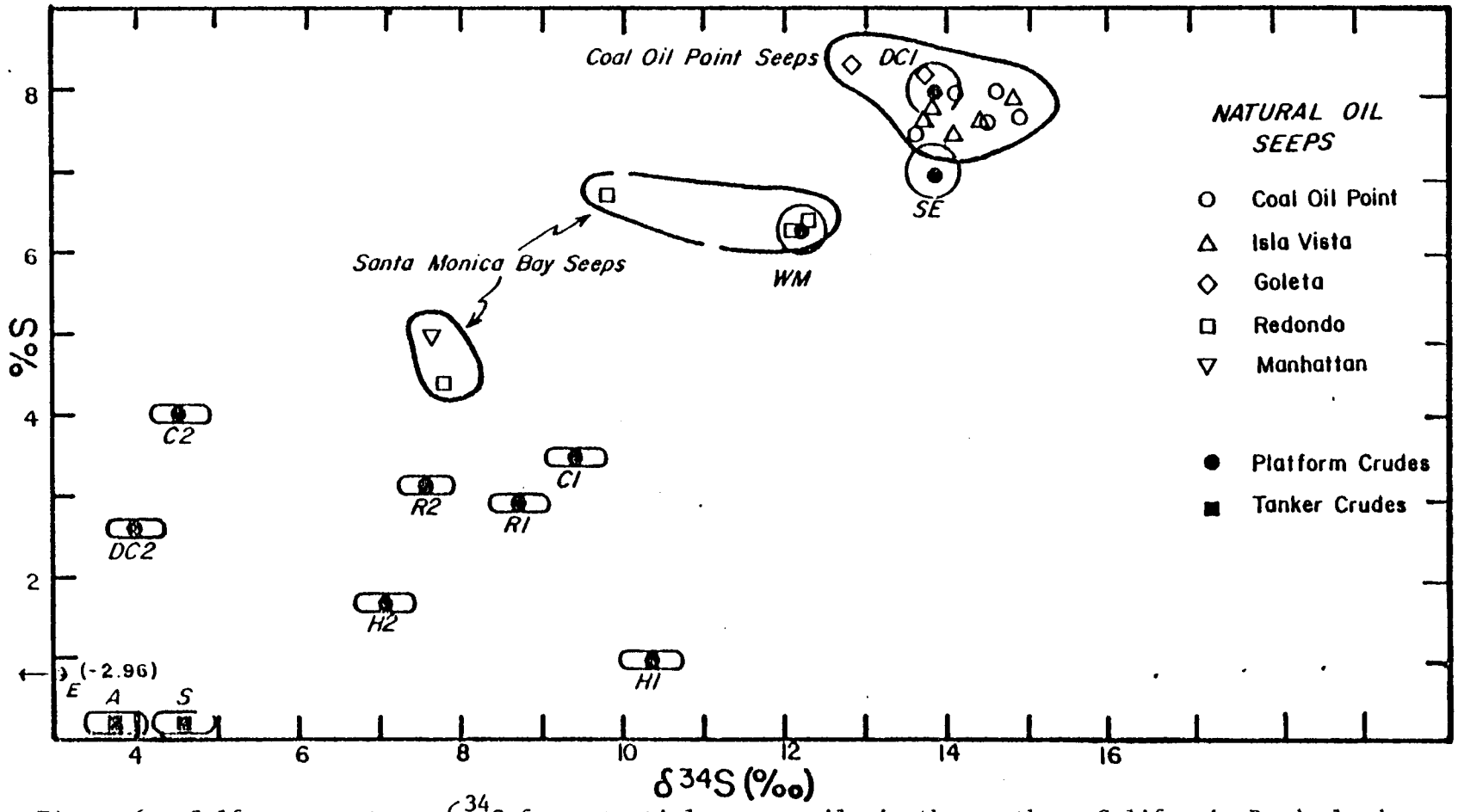

Figure 6. Sulfur content vs $\delta^{34}S$ for potential source oils in the southern California Borderland. Analytical precision represented by field areas. C1: Carpinteria, C2: Carpinteria 012, DC1: Dos Cuadras Platform Hillhouse, DC2: Dos Cuadras Platform A, E: Elwood, R1: Rincon PRC 145.1, R2: Rincon 145 #6, SE: South Elwood, WM: West Montalvo, H1: Huntington Beach #J-50, H2: Huntington Beach, A: Arabian crude, S: Sumatran crude. Number in parentheses represents values for oils which lie outside the scale of the diagram.

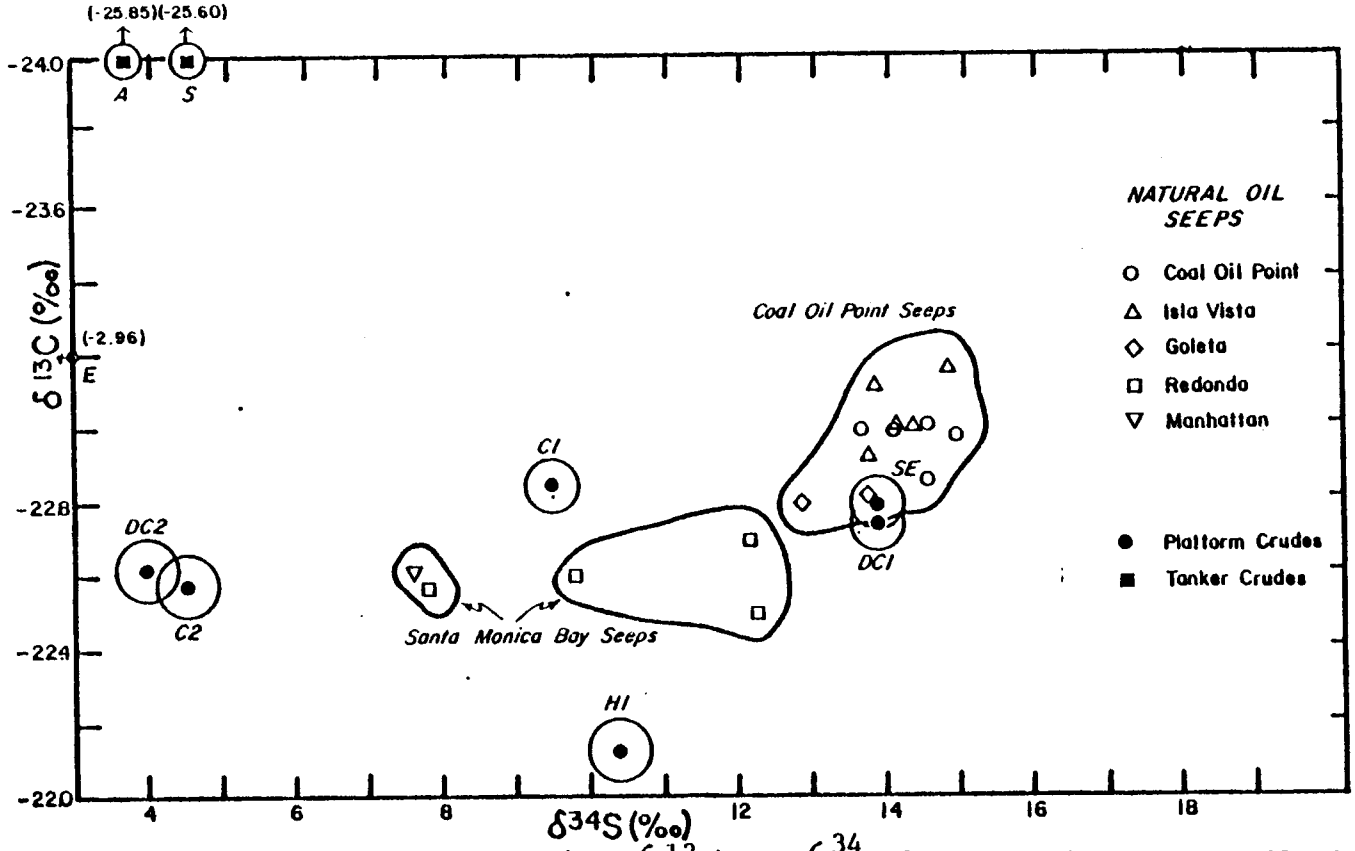

Figure 7. Carbon isotope ratio (as $\delta^{13}C$) vs $\delta^{34}S$ for potential source oils in the southern California borderland. Analytical precision represented by field areas. C1: Carpinteria, C2: Carpinteria 012, DC1: Dos Cuadras Platform Hillhouse, DC2: Dos Cuadras Platform A, E: Elwood, SE: South Elwood, WM: West Montalvo, H1: Huntington Beach #J-50, A: Arabian crude, S: Sumatran crude. Numbers in parentheses represent values for oils which lie outside the scale of the diagram.

Formation, Oligocene) based on the three analyzed parameters, an unlikely source since the oldest strata in this area is Middle Miocene (Nardin, 1976).

Data from the weathering experiments are summarized in Table 3. The data from the controlled weathering simulation experiment are shown graphically in Figure 8.

The degree of weathering of the oils in the controlled experiment was inferred from the gas chromatograms (Figure 9) by normalizing the peak height of the major alkane compounds to the C-24 peak and defining a weathering index as:

$$W.I. = \frac{(C_i/C_{24}) \text{ weathered oil}}{(C_i/C_{24}) \text{ unweathered oil}}$$

Where C_i represents an alkane compound with i carbon atoms, for i equal to integers from 1 to 30.

The weathering index for the experimental oils is plotted against carbon number in Figure 10. A greater loss of the low molecular weight compounds is apparent in all three oils. The platform crude sample exhibits an apparent increase in compounds C-16 to C-21 after 33 days of weathering (Figure 10b). This increase may be a result of three processes: (1) the formation of these compounds from other fractions in the petroleum upon weathering; (2) contamination of the unweathered sample aliquot; (3) inclusion of bacterial cells (Sweeney, personal communication). The apparent decrease in the weathering index of compounds larger than C-24 in the Sumatran crude must be due to a loss of C-24 relative to larger compounds (Figure 10c).

Figure 11a illustrates the frequency of heavy tar deposition on

three beaches in Santa Monica Bay from August, 1975 to January, 1978. Figure 11b is a similar plot for the three stations at which tar samples were collected. On the average, tar density is at a maximum during the spring, summer, and fall seasons; but declines sharply during the three winter months of November, December, and January. This pattern is similar to the trend noticed by Ludwig and Carter (1961) for Torrance Beach.

The size of the surface slick observed by the U.S. Coast Guard overlying the Santa Monica Bay natural seepage zones is illustrated in Figure 12 for the same time period as the beach tar observations.

Table 3. Data from the controlled weathering and beach weathering experiments.

Sample	Exposure time (days)	$\delta^{13}C$ (‰)	%S	$\delta^{34}S$ (‰)
Controlled Weathering				
Sumatra Crude	0	-25.60	0.19	+ 4.70
	33	-25.59	0.20	+ 4.08
	50	-25.57	0.19	+ 4.16
	100		0.25	+ 4.16
Platform Crude	0	-22.24	1.96	+ 5.80
	33	-22.37	2.12	+ 6.76
	50	-22.44	1.95	+ 7.27
	100		2.24	+ 6.95
Seep Oil	0		7.57	+14.76
	42		7.72	+13.79
Beach Weathering				
Fresh #1		-22.83	--	--
Fresh #2		-22.89	7.71	+14.26
Weathered #1		-22.84	7.62	+14.36
Weathered #2		-22.79	--	+13.85
Highly Weathered #1		-22.88	7.63	+14.03

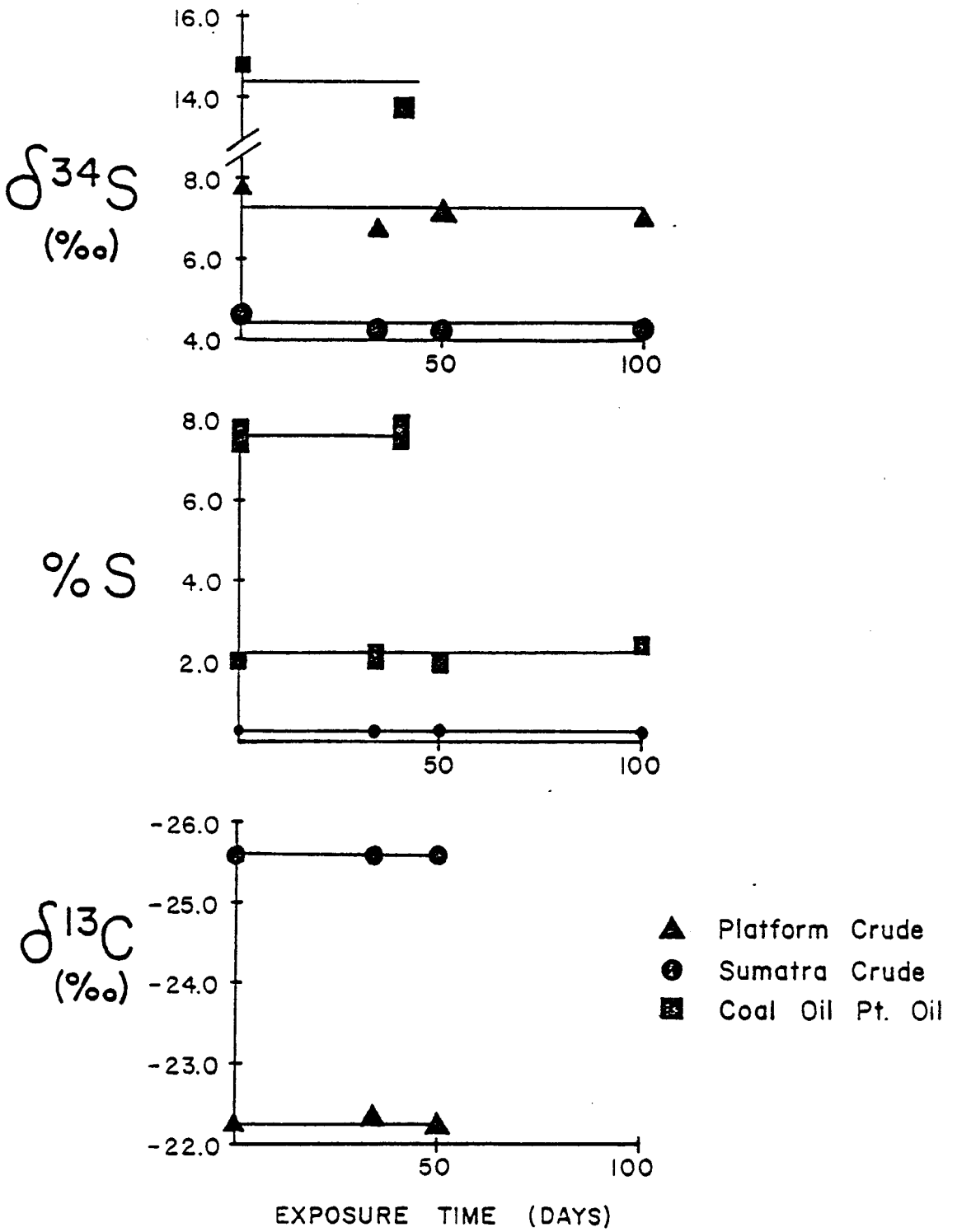

Figure 8. Data from the controlled weathering simulation experiment. Analytical precision represented by size of appropriate symbol.

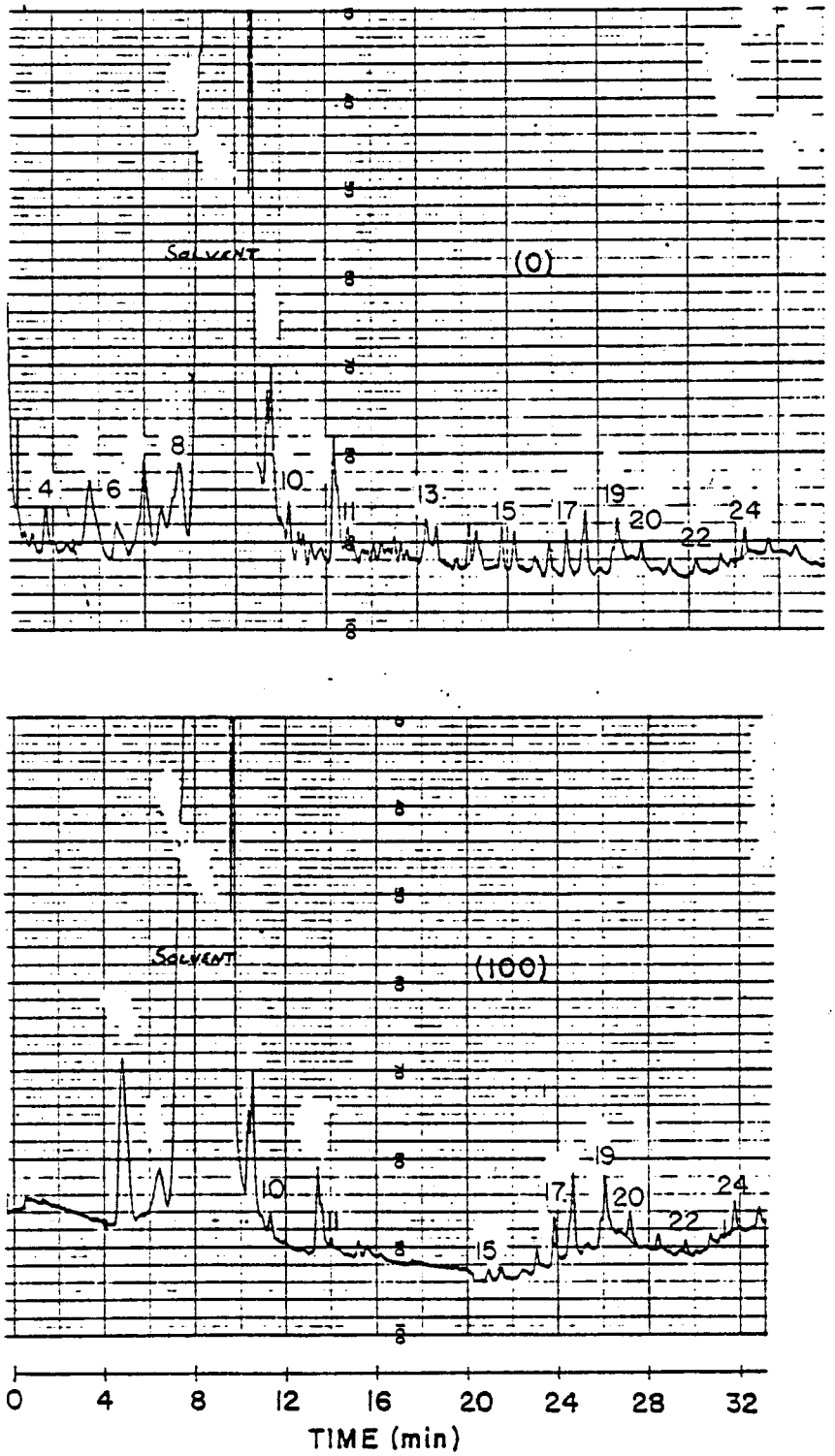

Figure 9a. Gas chromatograms of platform crude oil from the controlled weathering simulation experiment. Numbers in parentheses represent days of exposure. Electrometer set at 1 and 2 for range and attenuation, respectively.

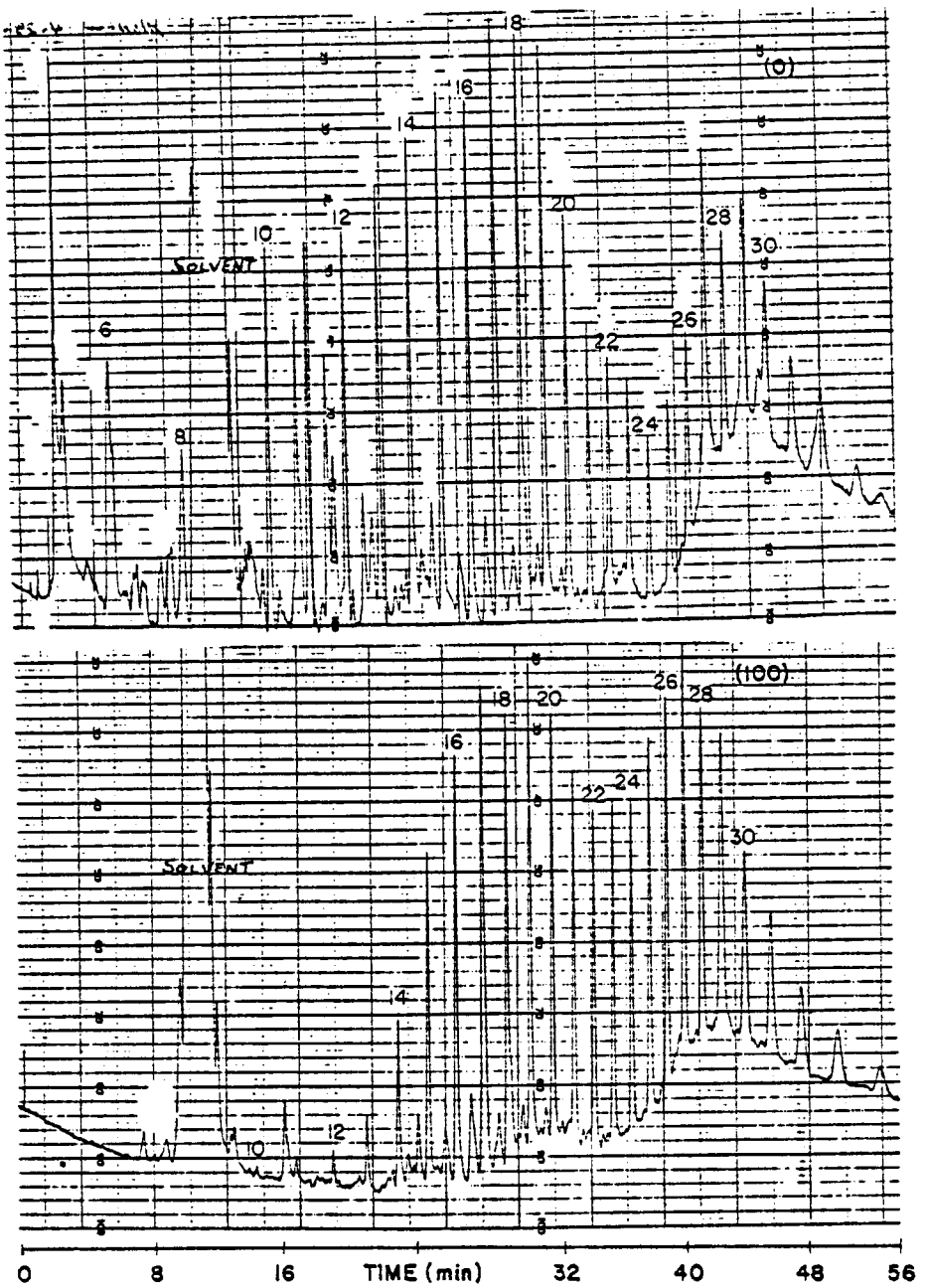

Figure 9b. Gas chromatograms of Sumatran crude oil from the controlled weathering simulation experiment. Numbers in parentheses represent days of exposure. Electrometer set at 1 and 2 for range and attenuation, respectively.

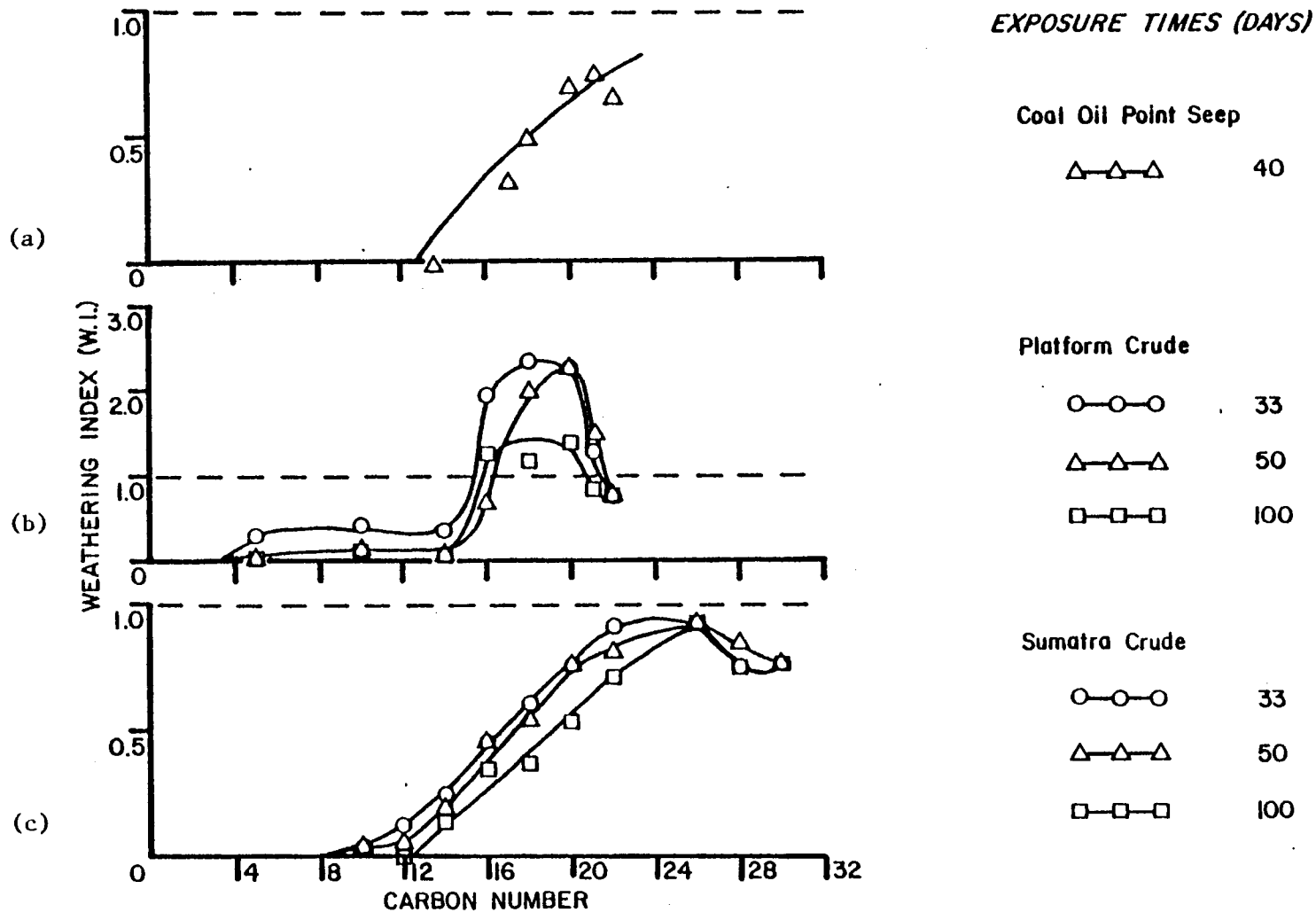

Figure 10. Weathering index vs carbon number for oils from the controlled weathering simulation experiment. (a) Seep oil, (b) Platform crude, and (c) Sumatra crude.

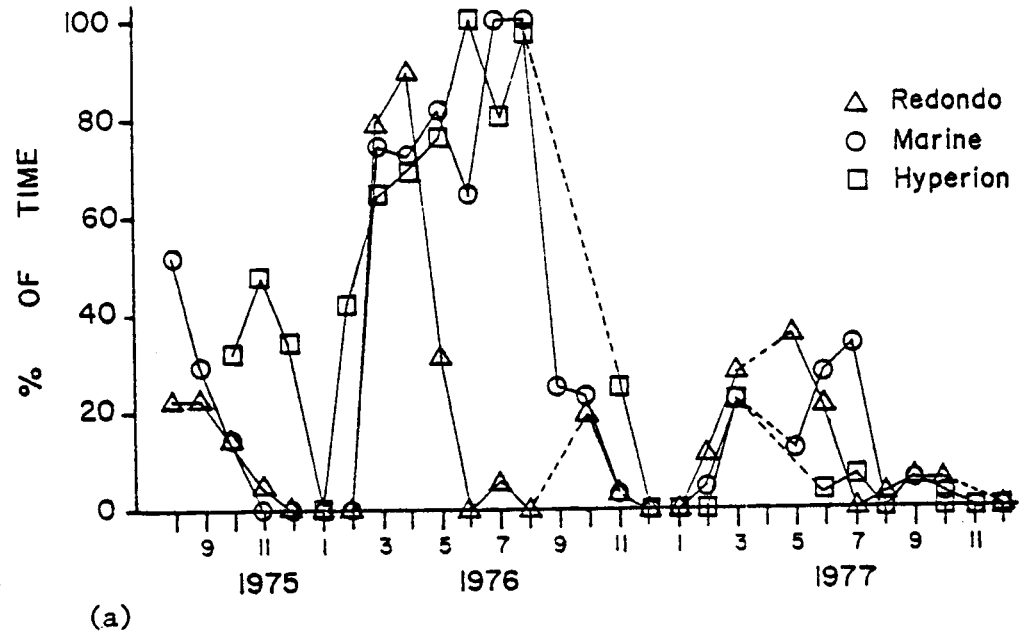

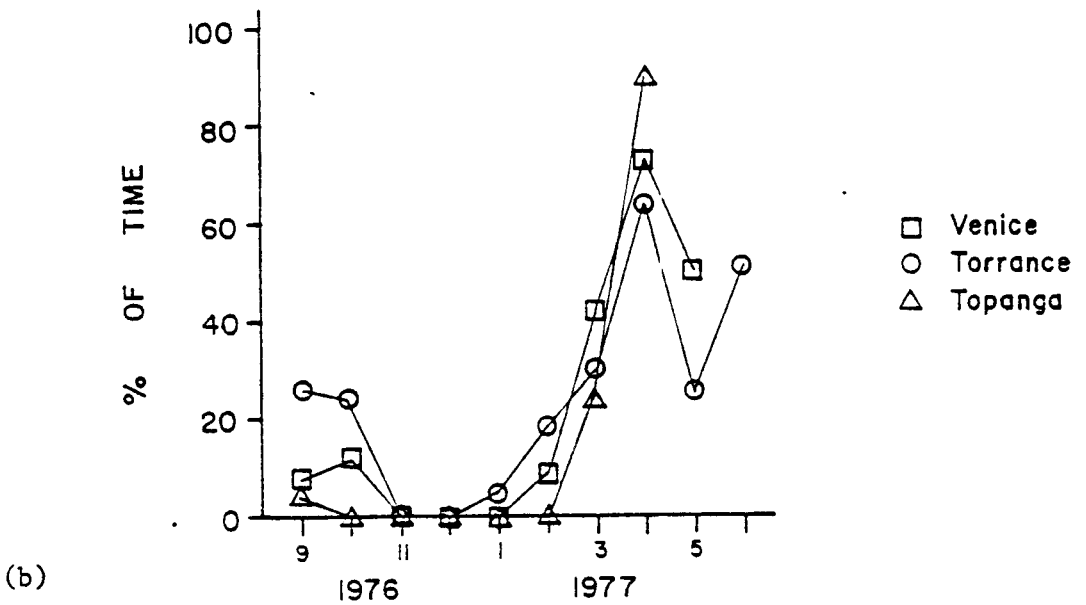

Figure 11. Frequency of heavy beach tar concentration (> 500 g per linear meter) for beaches in Santa Monica Bay. (a) Tar monitoring station and (b) tar sampling stations.

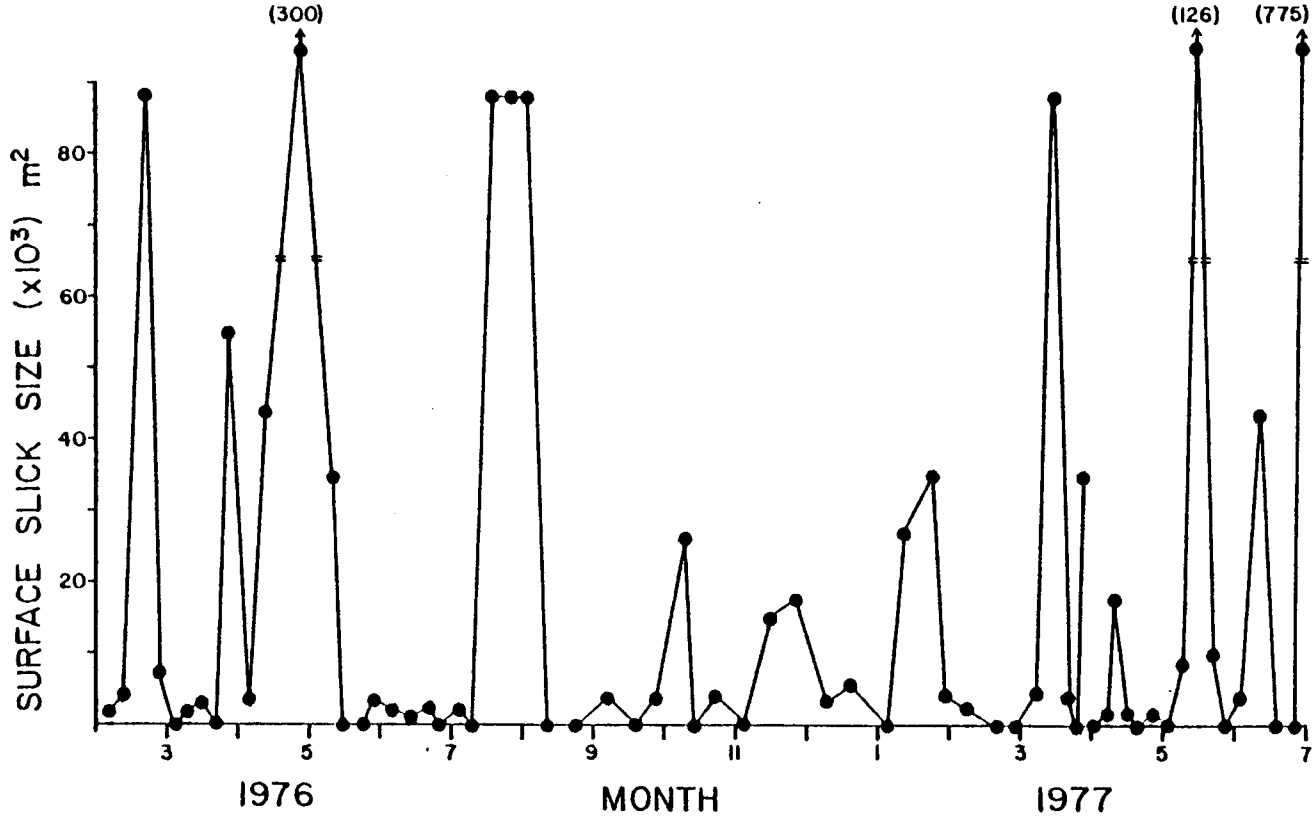

Figure 12. Surface slick size overlying the Santa Monica Bay natural oil seepage. Figures in parentheses represent slick size during periods of extremely high activity.

DISCUSSION

Source Identification of Beach Tars

The assumption that the asphaltene fraction of petroleum is insensitive to weathering processes is supported by the data obtained from the controlled weathering experiment. After 100 days of simulated weathering, during which most of the lighter fractions were lost, the three parameters measured in the asphaltene fraction did not vary by more than the limits of analytical precision. Data from the beach weathering experiment further support this conclusion.

The determination of the origin of the tars is best performed by comparing the chemistry of the tars to the chemistry of the possible source oils on two parameter plots (Figures 13 and 14). The majority of the beach tars analyzed fall within the areas corresponding to the natural seep oils. The %S vs. $\delta^{34}S$ plot (Figure 13) shows a good correlation between beach tars and oil from each of the natural seepages. The variation of these parameters between oils from the natural seepages enables tars originating from each seep to be differentiated. There is considerable scatter in the correlation of beach tars with the natural seep oils on the $\delta^{13}C$ vs. $\delta^{34}S$ plot (Figure 14), probably a result of the small variation in $\delta^{13}C$ relative to analytical precision. Thus, this plot is not sensitive to the small variations in $\delta^{13}C$ between the natural seep oils and cannot be used for tracing tars to a specific seep.

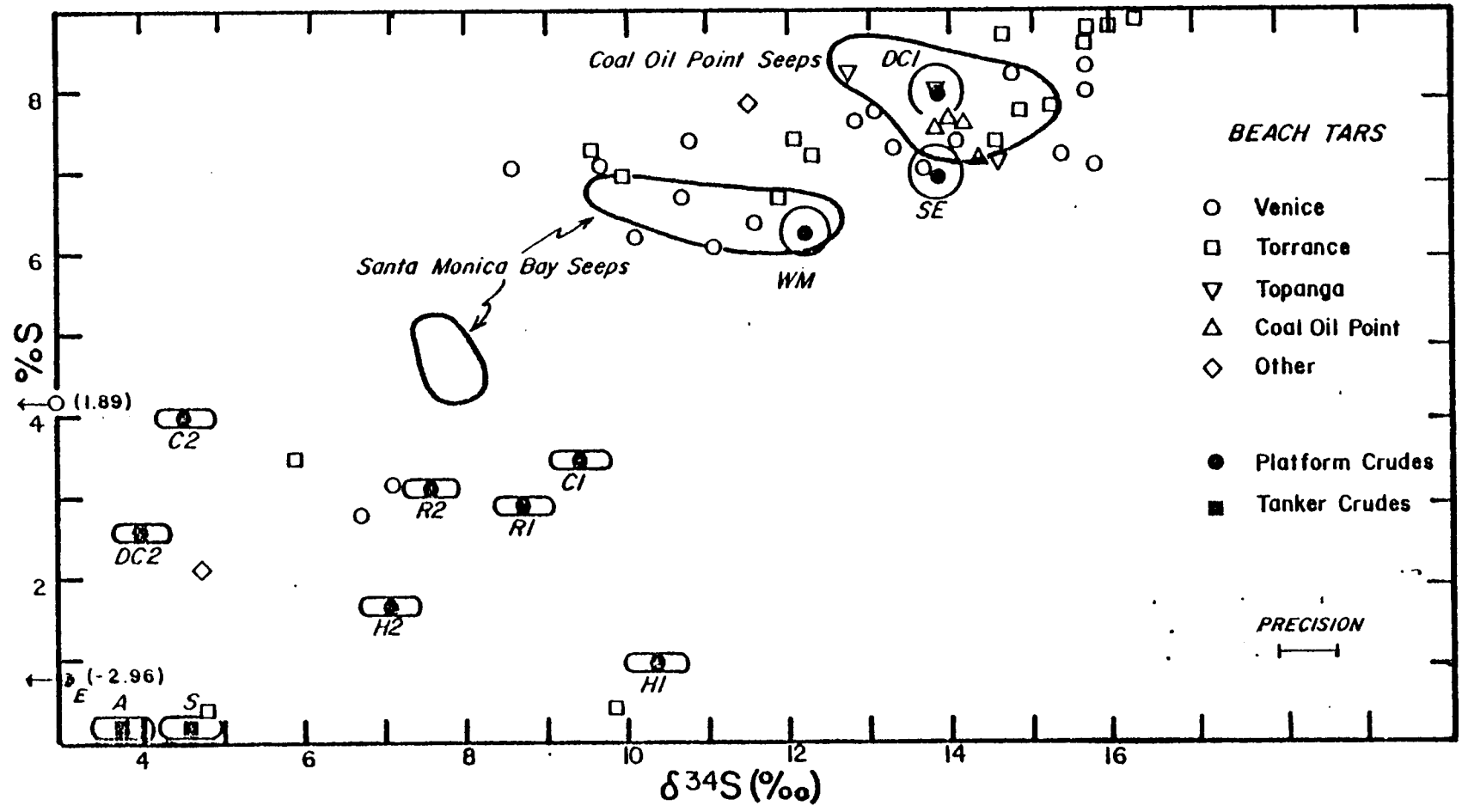

Figure 13. Sulfur content vs $\delta^{34}S$ for analyzed beach tars. Numbers in parentheses represent values which lie outside the scale of the diagram. Platform and tanker codes from Figure 6.

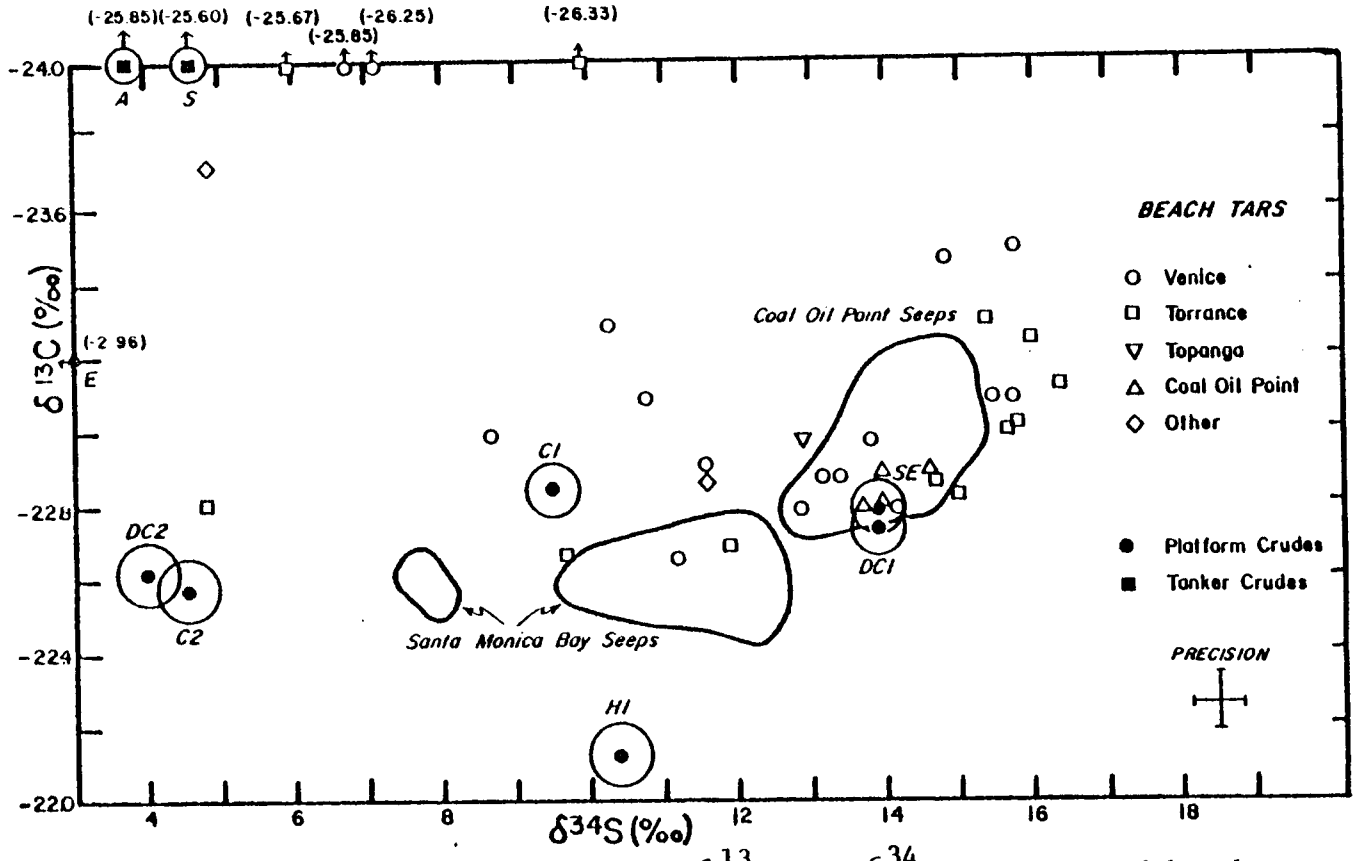

Figure 14. Carbon isotope ratio (as $\delta^{13}C$) vs $\delta^{34}S$ for analyzed beach tars. Numbers in parentheses represent values which lie outside the scale of the diagram. Platform and tanker codes from Figure 7.

On the basis of the %S vs $\delta^{34}S$ plot (Figure 13), it is inferred that approximately 82% of the tars found in Santa Monica Bay originate from natural oil seepage. The seepage at Coal Oil Point, located nearly 170 km to the northwest, supplies approximately 51% of the tars to the beaches. In contrast, the nearby Santa Monica Bay seeps supply only about 31% of the total (Table 4). Two of the tar samples in Figure 13 plot between the seep fields and cannot be traced to a specific seep, probably reflecting either contamination during transport from source to beach or analytical error.

Eighteen percent of the tars in Figure 13 do not resemble any of the potential source oils. These samples are of unknown origin and are summarized in Table 5. Four of the samples were found on the same day at two different beaches. Two of the remaining four samples were found at the same beaches three weeks later. These 6 tars also were similar in physical appearance. All were hard, thick (2-3 cm.) tars, closely resembling a roof asphalt. Tars similar to these have been observed on beaches in Santa Monica Bay during previous years, but only during the fall season. It is possible that these tars might originate from an unknown natural seep or man-induced source which is located in a position where tar transport to the beaches is possible only during the fall season due to current variations.

The other two unknown tars were unconventional samples in that their physical properties, such as texture and smell, were distinctly different from the average tar lumps. The Blacks Beach (5-19-77) sample was collected nearly 200 kilometers southeast of Santa Monica Bay during a single episode of tar deposition. This sample differed from common

Table 4. Origin of tars in Santa Monica Bay based on %S, $\delta^{34}S$, & $\delta^{13}C$.

Source	# of Samples	Tars supplied (%)
Coal Oil Point Seepage	22	51
Santa Monica Bay Seepage	13	31
Unknown	8	18

Table 5. Carbon isotope ratio (as $\delta^{13}C$), %S, and $\delta^{34}S$ of unidentified tars found in Santa Monica Bay.

Sample	$\delta^{13}C$(‰)	%S	$\delta^{34}S$(‰)
Torrance 9-20-76 (1a)	-25.67	3.50	+ 6.02
Venice 9-20-76 (10a)	-25.85	2.60	+ 6.79
Venice 9-20-76 (10b)	-26.07	2.50	--
Venice 9-20-76 (10c)	-24.02	5.46	--
Venice 10-01-76 (10c)	-26.25	3.20	+ 7.17
Torrance 10-7-76 (1b)	-22.82	0.44	+ 4.86
Blacks 5-19-77 (50a)	-23.73	2.15	+ 4.88
Venice 6-11-77 (10c)		4.20	+ 1.80

beach tar samples by its unusual "sweet" smell, a characteristic of low sulfur crudes. The source is believed to be a passing tanker although this conclusion cannot be substantiated without a matching source oil. The Venice Beach (6-11-77) sample was unusual in that it resembled an oil-rich sand. No predictions of its source were attempted.

The $\delta^{13}C$, %S, and $\delta^{34}S$ of individual tar lump samples and a bulk sample, consisting of an aggregate of lumps found on the beach, collected on the same day are listed in Table 6. The data support the hypothesis that tar deposited on beaches on any given day can be derived from more than one source. Homogenization of the tar lumps upon collection may result in a loss of sensitivity and error on the source determination. No correlations were observed between tar lump size and origin.

Pathways of Transport

Figure 15 illustrates the relative contribution from the potential sources of tar found on three beaches in Santa Monica Bay from September, 1976 to July, 1977 on days of heavy tar concentration. A correlation between the amount of tar derived from the Coal Oil Point seeps and beach tar concentration is apparent upon comparison with Figure 11b. The periods of heaviest tar concentration on beaches in Santa Monica Bay occur when the majority of tars are derived from the Coal Oil Point seepage regardless of season. No simple correlation appears to exist between the Santa Monica Bay seepage flow rate and tar density on local beaches.

The sharp reduction in the tar concentration on Santa Monica Bay beaches during the winter months (Figure 11) apparently reflects a decline in tar from Coal Oil Point reaching this segment of coastline.

Table 6. Analyses of individual tar lumps and bulk sample collected on same day.

Location	Date	$\delta^{13}C$ (‰)	%S	$\delta^{34}S$ (‰)	Probable Source
Venice Beach	10-1-76				
Lump #1		-26.25	3.20	+ 7.17	Unknown
Lump #2		-23.30	6.19	+10.23	Santa Monica Bay Seep
Bulk		-23.51	8.04	+15.85	Coal Oil Point Seep
Torrance Beach	4-9-77				
Lump #1		-22.69	7.28	+ 9.71	Santa Monica Bay Seep
Lump #2		-22.70	6.71	+11.96	Santa Monica Bay Seep
Lump #3		-23.06	8.79	+15.85	Coal Oil Point Seep
Bulk		-22.98	8.60	+15.67	Coal Oil Point Seep

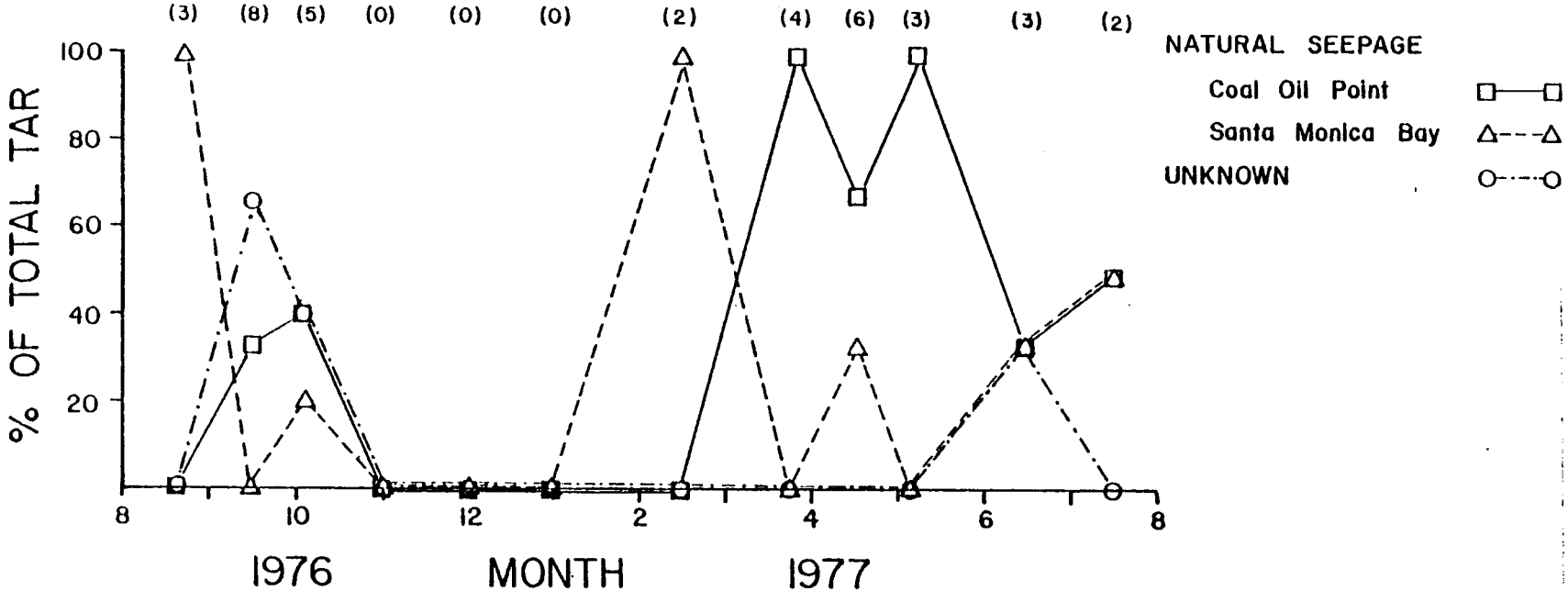

Figure 15. Relative contribution of beach tar found on three beaches in Santa Monica Bay from the potential sources. Numbers in parentheses represent number of tar samples analyzed each month.

The lower contribution of tar from this seepage area during the winter months may be explained by examining the transport of tar from Coal Oil Point to Santa Monica Bay.

The circulation in the southern California Borderland is bounded by the coastline to the north and east and the California current on the west. Within these boundaries three major gyres are developed. The southern California gyre extends from Point Conception to Baja, Mexico (Schwartzlose and Reid, 1972). Two smaller gyres also exist, one in the Santa Barbara Channel (Kolpack, 1971) and a complex one in Santa Monica Bay (Stevenson et al., 1956). The overall pattern is highly variable and may exhibit daily, as well as seasonal, change (Figure 16a).

Oil seeping from Coal Oil Point has two potential pathways to Santa Monica Bay, a westerly path or an easterly path. It may initially drift westward in the Santa Barbara Channel gyre past Point Conception and towards the eastern limit of the California current, or it may initially move easterly in the littoral currents to the Anacapa passage and return westward in the major channel gyre to enter the California current (Figure 16b). Once in the vicinity of the California current, the tar is carried southward and transported to Santa Monica Bay by the southern California gyre. Alternatively, tar may remain in the easterly directed littoral currents and drift through the Anacapa passage towards Santa Monica Bay (Figure 16b).

It is not possible to determine which one of the two potential directions is the actual pathway followed by the majority of tar found in Santa Monica Bay. O'Neil (1978) suggests that the predominant pathway is the littoral drift past Oxnard; however, there are currently no

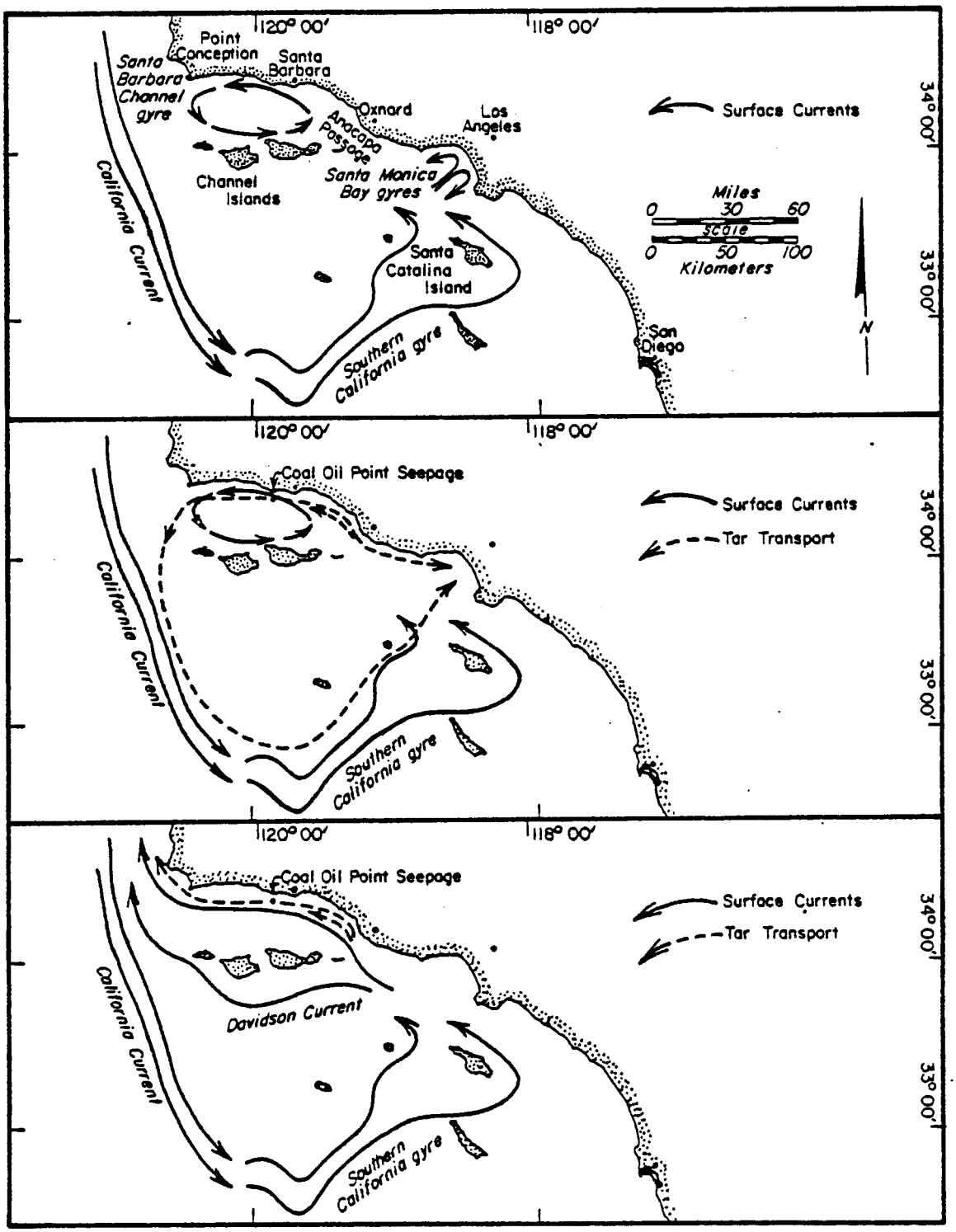

Figure 16. (a) General surface circulation in the southern California Borderland during the spring, summer, and early fall seasons, (b) possible transport pathways for tar from Coal Oil Point during the spring, summer, and early fall seasons, and (c) during the winter season.

data to support this hypothesis. A more conclusive model might be developed by studying the tar distribution on the offshore islands and along the California coastline from Oxnard to Point Dume.

During the winter months, the borderland circulation changes as the California undercurrent, commonly referred to as the Davidson current, surfaces in the vicinity of the Channel Islands and flows in a northwesterly direction through the Santa Barbara Channel and around Point Conception (Schwartzlose and Reid, 1972) (Figure 16c). Tars that originate from Coal Oil Point are trapped in the Davidson current during the winter months and flow towards the north, away from Santa Monica Bay, depositing on the California coastline north of Point Conception (Figure 16c). This northward transport has been observed by Schwartzlose (1963) using drift cards. Beach tars with sulfur concentrations similar to oil from the Coal Oil Point seeps have been found north of Point Conception during January, 1978, further supporting this pattern.

The time for tar to travel from the Santa Barbara Channel to Santa Monica Bay may be calculated as:

$$\tau = \frac{\text{distance traveled}}{\text{drift rate}}$$

The travel distance may be assumed as 250 kilometers. The drift rate may be taken as close to that of the California current (20-30cm/sec). Substituting these values:

$$\tau = \frac{250 \text{ km}}{20\text{-}30 \text{ cm/sec}} = 10\text{-}14 \text{ days.}$$

This value is in close agreement with drift times determined by Kolpack (personal communication) based on drift card studies in the Santa

Barbara Channel.

Field estimates of the residence time of the tar lumps in the surface ocean were made possible by the collection of tar lumps during the spring containing numerous goose barnacles. Horn et al. (1970) determined that this species of barnacle, Lepas (Lepas), attaches to floating objects in its planktonic larval stage and subsequently grows at a rate of 1-2 mm/week. Barnacles observed on the tar in Santa Monica Bay ranged in size from 2 to 7 mm, indicating a minimum residence time in water of 1 to 5 weeks, which is in good agreement with the calculated value.

Although the contribution of tar to beaches in Santa Monica Bay from the Santa Monica Bay seeps is not as large as tar contributed from the Coal Oil Point seeps, it represents a significant input. The transport of this tar is also poorly understood. Allen et al. (1971) attempted to quantify tar transport from these seepages by drift card measurements. They concluded that oil and tar drift from the seep to the coastline within an average of 5 days.

The slick mass overlying the Santa Monica Bay seeps can be calculated from the slick size by estimating the film thickness from visual appearance of the slick (Allen and Schlueter, 1969). Figure 17 illustrates the relationship between mass of oil in the surface slick and the contribution of beach tars from these seeps from August, 1976 to July, 1977. Although estimates of slick mass can be made from the available data only four times per month, there appears to be a reasonable correlation between periods of large slick mass ($>$ 10 kg) and periods of tars attributed to the Santa Monica Bay seeps found on

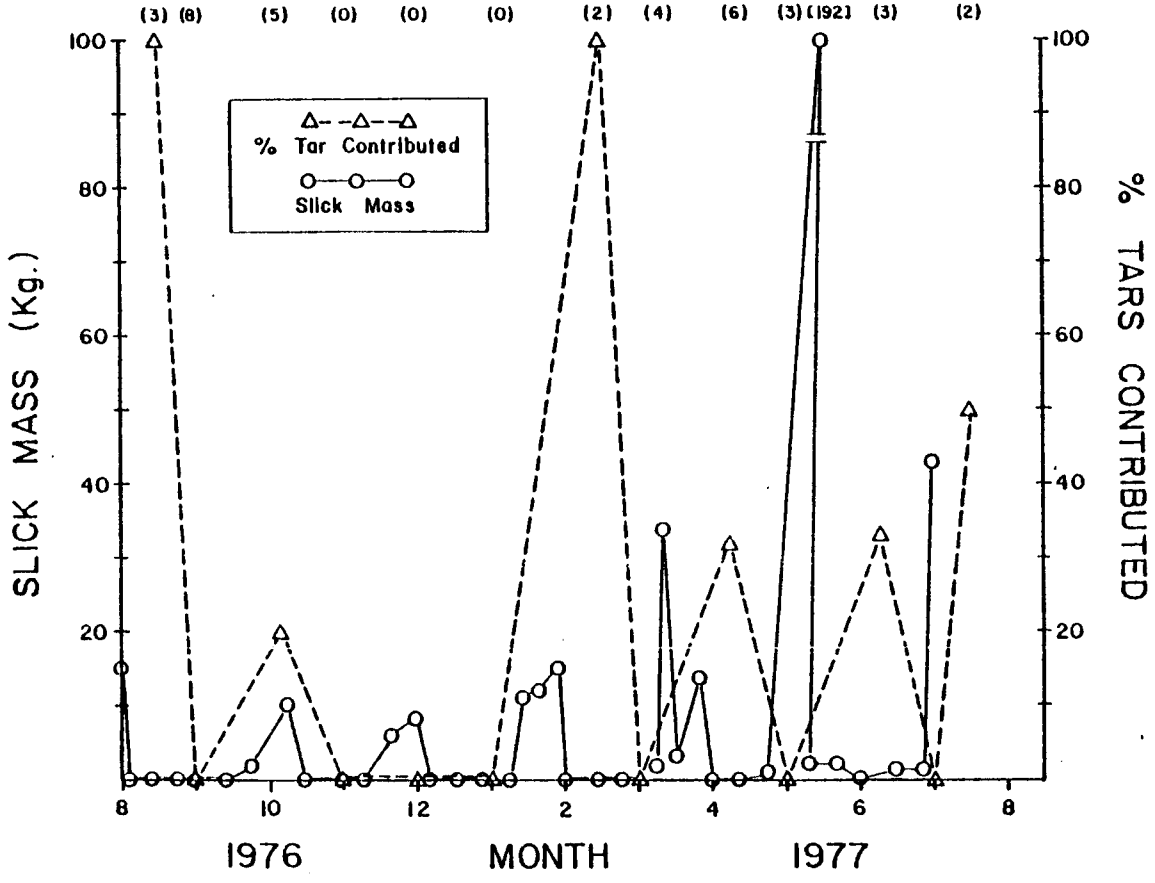

Figure 17. Mass of the slick overlying the Santa Monica Bay natural oil seepage and contribution of tars on neighboring beaches from the Santa Monica Bay seeps. Number in brackets represents size of slick mass during extremely high activity. Numbers in parentheses represent number of tar samples analyzed each month.

neighboring beaches. The drift time for tars derived from this seepage to the local beaches is given by the lag period between the two curves plotted in Figure 17. During the period from August, 1976 to July, 1977, when the slick mass exceeded 10 kg, the lag period before tars were found on local beaches ranged from 10 to 20 days, significantly longer than the 5-day drift time determined by Allen et al. (1971). The longer drift time suggests that the tar lumps do not take a direct path from seep to shore.

The surface circulation in Santa Monica Bay is dominated by a net inflow of water from the west which sets up a slow counter-clockwise motion in the northern half of the bay and a slow clockwise motion in the southern half, the magnitude and location exhibiting seasonal dependence (Gorsline, personal communication). In addition, narrow channels of relatively rapid offshore transport of water exist at depths of up to 50 m throughout the bay (Kolpack, personal communication). It is possible that this offshore transport of water extends to the surface and that tar forming above the Santa Monica Bay seepage zones is entrapped in the net outflow of surface water, moving in a gyral motion around the bay before drifting ashore (Figure 18). The number of revolutions each tar lump makes depends on the size of the gyre and the strength of the surface currents. Tar continues to circulate in the gyre until a change of oceanographic or meteorological conditions, such as wind direction or tidal amplitude, cause a breakdown in the gyral motion. The tar is then transported shoreward or completely out of the bay. Attempts to substantiate this model by relating wind direction and intensity, and swell direction to periods

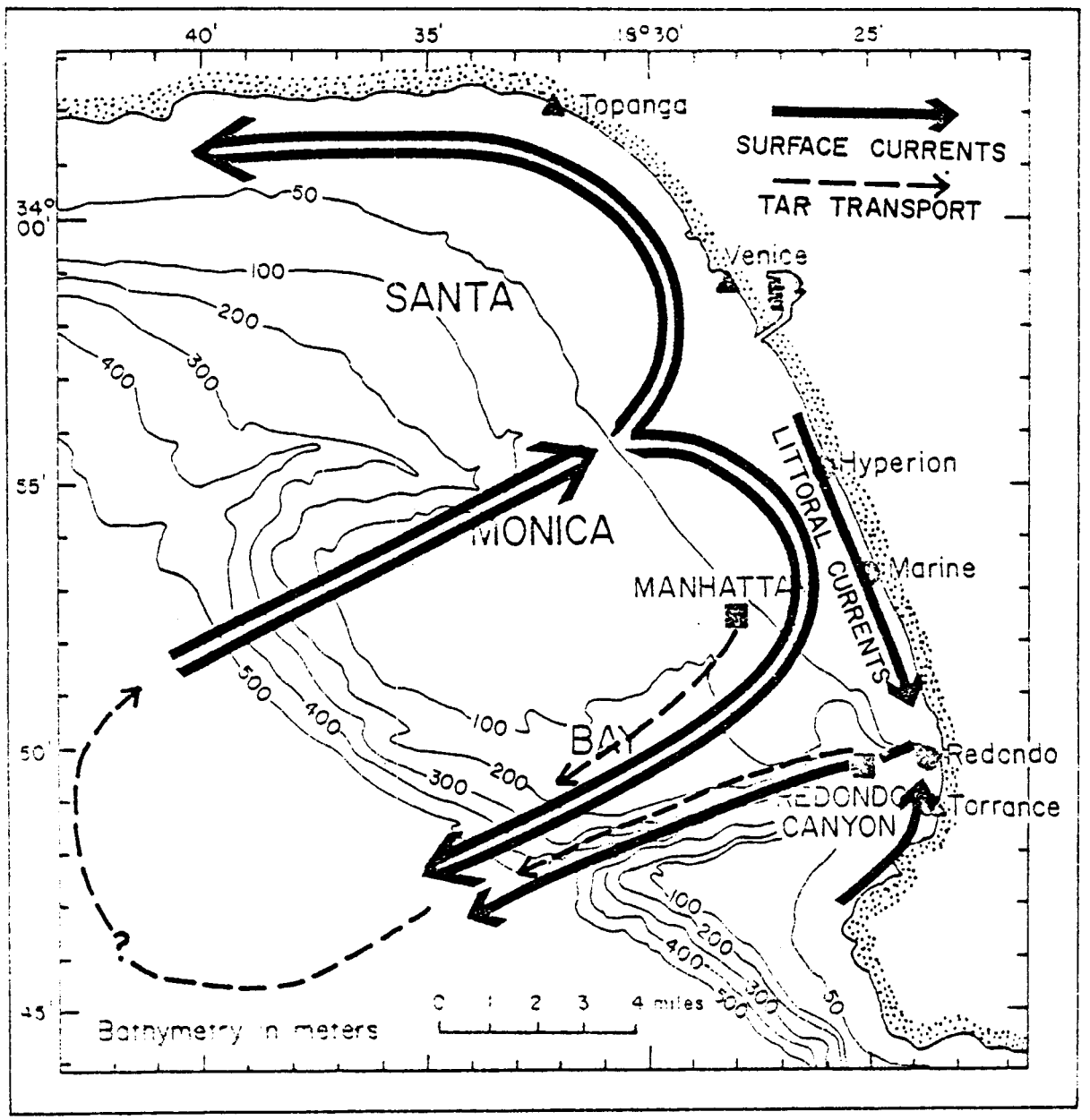

Figure 18. Simplified patterns of surface circulation in Santa Monica Bay and possible patterns of tar transport from the Santa Monica Bay seepages to nearby beaches.

of tar deposits, proved inconclusive.

Tar concentrations from the Santa Monica Bay seeps found on neighboring beaches are a function of the seepage rate and offshore current patterns. The size of the mass in the overlying slick appears to decline during the period from September, 1976 to January, 1977, possibly indicating a variation in seep rate during the winter season or an increase in surface ocean turbulence. This correlates with the absence of tar attributed to this seepage found on local beaches during the same period.

Fates

The average residence time for tar lumps on a beach is in the range of 1-2 tidal cycles, deduced from visual observations. The percentage of time that tar deposition on beaches in Santa Monica Bay reaches heavy concentrations (> 500 g per meter of shore) may be estimated from Figure 11 to be about 20% of the year. Assuming that the coastline in the bay from Malibu to Torrance Beach (Figure 4), a distance of approximately 25 km, is uniformly contaminated, and that the average residence time of tar on the beach is 24 hours, the total quantity of tar depositing in the bay per year is:

$$\text{Amount of tar} = (365 \text{ days/yr})\ (.20)\ (500 \text{ g/m})\ (25 \text{ km})$$

$$\cong 9.2 \times 10^{8} \text{ g/yr}$$

The fraction of this tar originating from the Coal Oil Point seepage is:

$$(.51)\ (9.2 \times 10^{8} \text{ g/yr}) \cong 4.7 \times 10^{8} \text{ g/yr}.$$

Assuming an average seepage flow rate of 70 barrels/day (Mikolaj et al., 1972), the tar depositing in Santa Monica Bay represents:

$$\frac{4.7 \times 10^8 \text{ g/yr}}{3.8 \times 10^9 \text{ g/yr}} \simeq 12\% \text{ of the Coal Oil Point seepage flow}$$

rate.

The fraction of tar derived from the Santa Monica Bay seeps is:

$$(.31)\ (9.2 \times 10^8 \text{ g/yr}) \simeq 2.8 \times 10^8 \text{ g/yr.}$$

Assuming an average seepage flow rate of 15 barrels/day (Wilkinson, 1971), this tar represents:

$$\frac{2.8 \times 10^8 \text{ g/yr}}{8.3 \times 10^8 \text{ g/yr}} \simeq 34\% \text{ of the Santa Monica Bay seepage}$$

flow rate.

Estimates of the loss of volatile components from petroleum during weathering range from 15% (Allen et al., 1971) to approximately 50% (Kolpack, personal communication) of the initial slick mass. Thus, the tar depositing in Santa Monica Bay represents approximately 14% to 24% of the total tar input from the Coal Oil Point seeps and 40% to 68% of the tar input from the Santa Monica Bay seeps. A larger proportion of the tar from the Santa Monica Bay seeps deposits on beaches in the bay, an expected result owing to the proximity of these seeps. Combining the previous calculations, the tar depositing in Santa Monica Bay represents:

$$\frac{7.5 \times 10^8 \text{ g/yr}}{4.7 \times 10^9 \text{ g/yr}} \simeq 16\% \text{ of the total seepage flow rate.}$$

Tar transported onto the shore typically agglomerates large quantities of sand, reaching densities greater than that of seawater. The dominant fate of beach tar is offshore transport by bottom currents. Tar depositing in Santa Monica Bay is probably transported down the 3 submarine canyons and off the shelf edge into the bordering Santa

Monica Basin. Kolpack (1971) predicted a similar mechanism of transport of heavy petroleum deposits into the Santa Barbara Basin after the 1969 Santa Barbara oil spill.

Assuming that all of the beach tar depositing in Santa Monica Bay is transported to the Santa Monica Basin, the sedimentation rate of petroleum hydrocarbons in the basin may be determined as:

$$\text{Rate of hydrocarbon deposition} = \frac{\text{total input of tar}}{\text{surface area of basin}}$$

The tar input into the basin from natural oil seepage is 7.5×10^8 g/yr. Assuming that the majority of tar settles in the flattest portion of the Santa Monica Basin, the effective surface area may be estimated from the basin dimensions below the 800 m depth contour as:

$$(33 \text{ km})\ (50 \text{ km}) = 1650 \text{ km}^2 = 1.65 \times 10^{13} \text{ cm}^2$$

Then the rate of hydrocarbon deposition is:

$$R = \frac{7.5 \times 10^8 \text{ g/yr}}{1.65 \times 10^{13} \text{ cm}^2} = 45\ \mu\text{g/cm}^2\text{-yr}$$

This result is approximately 3 times greater than measured deposition rates of total hydrocarbons of 14 μg/cm^2-yr in this basin (Emery, 1960, p. 254). The disagreement between the calculated and observed values may be a result of degradation losses of petroleum after incorporation into the basin sediment (Kolpack, personal communication).

CONCLUSIONS

The stable isotopic ratios of carbon and sulfur and the total sulfur content in the asphaltene fraction of petroleum are insensitive to weathering processes. This enables the use of these parameters as chemical fingerprints for highly weathered petroleum in the marine environment. Applying these parameters to the problem of the origin of tar on beaches in the greater Los Angeles area and correlating the chemical data with seasonal records of tar deposition and seep activity, the following conclusions were reached.

(1) The total sulfur content (%S) and sulfur isotopic ratio ($\delta^{34}S$) enable petroleum from the Coal Oil Point seepage area to be differentiated from petroleum seeping from the Santa Monica Bay natural oil seeps. The carbon isotopic ratio ($\delta^{13}C$) does not exhibit a wide variation among seep oils and is not as sensitive for distinguishing oils from the different seepages.

(2) The values of $\delta^{13}C$, %S, and $\delta^{34}S$ in the asphaltene fraction of oil seeping from the Isla Vista, La Goleta, and Coal Oil Point seepage zones are similar. The values of the parameters indicate that this oil is leaking from the Middle Miocene, Monterey Shale.

(3) The values of $\delta^{13}C$, %S, and $\delta^{34}S$ in the asphaltene fraction of oil seeping from the Manhattan and Redondo Canyon seepage zones are similar, but exhibit a temporal variation in chemistry. These parameters do not identify the source strata of these seeps.

(4) On the basis of $\delta^{13}C$, %S, and $\delta^{34}S$, oils from the natural seeps are distinguishable from the majority of crudes produced from the southern California Borderland and from tanker crudes imported into Santa Monica Bay from Arabia and Sumatra.

(5) Approximately 51% of the tars found in Santa Monica Bay are derived from the Coal Oil Point natural oil seepage, 31% from the seeps in Santa Monica Bay, and 18% from undetermined sources. Efforts to reduce contamination of the beaches by tar deposits should concentrate on stopping the flow of oil from the natural seeps.

(6) Seventy-five percent of the undetermined beach tars had similar chemical properties; possibly indicating a major unidentified input of petroleum into the coastal ocean.

(7) Tars identified as originating from Coal Oil Point are less abundant on Santa Monica Bay beaches during the months of November, December, and January. This decrease in tar concentrations may be attributed to the northwestward transport of tar in the Davidson current.

(8) Tars identified as originating from the Santa Monica Bay seepage often have a longer residence time in the surface water than predicted from drift card measurements, indicating the existence of a gyral circulation pattern in the southern part of Santa Monica Bay.

(9) Tar depositing in Santa Monica Bay represents approximately 40% to 68% and 14% to 24% of the total tar input into the ocean from the Santa Monica Bay seepage and Coal Oil Point seepage, respectively. Thus, deposition of tar on shore is a major fate for oil released from natural oil seeps in the southern California Borderland.

(10) Estimates of petroleum hydrocarbon sedimentation rates due to beach tar deposition in the Santa Monica Basin compare favorably with previously measured values for total hydrocarbons, suggesting that the Santa Monica Basin is the major sink for beach tars found in Santa Monica Bay.

REFERENCES

Adlard, E. R., 1972, A review of the methods for the identification of persistent hydrocarbon pollutants in seas and beaches: Jour. Inst. Petroleum, v. 58, p. 63-72.

Allen, A. A., and R. S. Schlueter, 1969, Estimates of surface pollution resulting from submarine oil seeps at Platform A and Coal Oil Point: Tech. Mem. 1230, General Research Corporation, Santa Barbara, Calif., p. 1-43.

Allen, A., L. Fausak, V. Sutherland, P. Mikolaj, and R. Schlueter, 1971, Santa Monica Bay natural oil seep investigation: Marconsult Inc. Technical Report, Standard Oil Company of California (Western Operations), 93 p.

American Society for Testing and Materials, 1961, Standard Method for Distillation of Petroleum Products, 8 p.

Bailey, S. A., and J. W. Smith, 1972, Improved method for the preparation of Sulfur Dioxide from Barium Sulfate for isotopic ratios studies: Anal. Chem., v. 44, p. 1542-1543.

Betancourt, O. J., and A. Y. McLean, 1973, Changes in chemical composition and physical properties of a heavy residual oil weathering under natural conditions: Jour. Inst. Petroleum, v. 59, p. 223-230.

Blumer, M., and J. Sass, 1972, The West Falmouth Oil Spill: Woods Hole Oceanographic Institution Tech. Report 72, Woods Hole, Mass., 125 p.

Blumer, M., M. Ehrhardt, and J. H. Jones, 1973, The environmental fate of stranded crude oil: Deep Sea Research, v. 20, p. 239-259.

Brunnock, J. V., D. F. Duckworth, and G. G. Stevens, 1968, Analysis of beach pollutants: Jour. Inst. Petroleum, v. 54, p. 310-325.

Chapin, D. W., 1972, Source identification of tar deposits from the Santa Barbara Channel coastline by trace metal analysis: M.S. Thesis, Univ. of Calif., Santa Barbara, Calif.

Claypool, G. E., 1974, Anoxic Diagenesis and Bacterial Methane Production in Deep Sea Sediments: PHD Dissertation, University of Calif., Los Angeles, Calif., 276 p.

Craig, H., 1957, Isotopic standards for carbon and oxygen and correction factors for mass-spectrometric analysis of carbon dioxide: Geochim. et Cosmochim. Acta., v. 12, p. 133-149.

Delaney, R. C., 1972, Trace metal weathering effect and characterization of oily pollutants from the Santa Barbara Channel: M.S. Thesis, Univ. of Calif., Santa Barbara, Calif.

Ehrhardt, M., and M. Blumer, 1972, The source identification of marine hydrocarbons by gas chromatography: Environ. Poll., v. 3, p. 179-194.

Emery, K. O., 1960, The sea off southern California: New York, John Wiley & Sons, 366 p.

Fischer, P. J., and R. Berry, 1973, Environmental hazards of the Santa Barbara Channel: oil and gas seeps and Holocene faulting, in Moran et al., eds., Geology, Seismisity, and Environmental Impact, Assoc. Eng. Geol., Spec. Pub., p. 417-431.

Horn, M. H., J. M. Teal, and R. H. Backus, 1970, Petroleum lumps on the surface of the sea: Science, v. 168, p. 245-246.

Jeffrey, P. J., 1973, Large-scale experiments on the spreading of oil at sea and its disappearance by natural factors: Proc., Joint Conf. on Prev. and Control of Oil Spills, Am. Petroleum Inst., Washington, D.C., p. 469-474.

Kaplan, I. R., J. W. Smith, and E. Ruth, 1970, Carbon and sulfur concentration and isotopic composition in Apollo 11 lunar samples: Proc. of the Apollo 11 Lunar Sci. Conf., v. 2, p. 1317-1329.

Kinney, P. J., D. K. Button, and D. M. Schell, 1969, Kinetics of dissipation and biodegredation of crude oil in Alaska's Cook Inlet: Proc. Join Conf. on Prev. and Cont. of Oil Spills, Am. Petroleum Inst., p. 333-340.

Kolpack, R. L., 1971, Biological and oceanographical survey of the Santa Barbara Channel oil spill, vol. II, Physical, chemical, and geological studies: Allan Hancock Foundation, Univ. Southern California, 477 p.

Kolpack, R. L., B. J. Mechalas, T. J. Meyers, N. B. Plutchak, and E. Eaton, 1973, Fate of oil in a water environment, vol. I, A Review and Evaluation of the literature: Am. Petroleum Inst., no. 4213, 73 p.

Koons, C. B., P. H. Monaghan, and G. C. Bayliss, 1971, Pitfalls in oil spill characterization: Needs for multiple parameter approach and direct comparison with specific parent oils: Presented at Southwest Regional ACS Meeting, San Antonio, Texas, December.

Koons, C. B., 1972, Chemical composition: a control on the physical and chemical processes acting on petroleum in the marine environment: Proc. Gulf Coast Assoc. Geologists Soc., Houston, Texas.

Kreider, R. E., 1971, Identification of oil leaks and spills: Proc. Joint Conf. on Prev. and Cont. of Oil Spills, Am. Petroleum Inst., p. 119-124.

Ludwig, H. F., and R. Carter, 1961, Analytical characteristics of oil-tar materials on southern California beaches: Jour. Water Poll. Cont. Fed., p. 1123-1140.

Merz, R. G., 1959, Determination of the quantity of oily substances on beaches and in nearshore waters: State of California Water Pollution Control Board, no. 21, 45 p.

Mikolaj, P. G., A. A. Allen, and R. S. Schlueter, 1972, Investigation of the nature, extent, and fate of natural oil seepage off southern California: Offshore Tech. Conf., no. 1549, Houston, Texas.

Monster, J., 1972, Homogeneity of sulfur and carbon isotope ratios $^{34}S/^{32}S$ and $^{13}C/^{12}C$ in petroleum: Am. Assoc. Petroleum Geologists Bull., v. 56, p. 941-949.

Nardin, T. R., 1976, Late Cenozoic History of the Santa Monica Bay Area: California: M.S. Thesis, Univ. South. Calif., Los Angeles, Calif., 189 p.

National Academy of Sciences, 1975, Petroleum in the Marine Environment: Washington, D.C., 197 p.

O'Neil, T. J., 1978, PhD dissertation, Univ. of So. Ca. - in prep.

Orr, W. L., 1974, Changes in sulfur content and isotopic ratios of sulfur during petroleum maturation - study of Big Horn Paleozoic oils: Am. Assoc. Petroleum Geologists Bull., v. 58, p. 2295-2318.

Parr Instrument Company, 1964, Oxygen bomb Colorimetry and combustion methods: Technical manual, no. 130.

Reed, W. E., and I. R. Kaplan, 1977, The chemistry of marine petroleum seeps: Jour. Geochem. Exp., v. 7, p. 255-293.

Sachanen, A. N., 1945, The chemical constituents of petroleum: New York, Reinhold Publishing Corp., N.Y., p. 385-313.

Sakai, H., 1957, Fractionation of sulfur isotopes in nature: Geochim. et Cosmochim. Acta., v. 12, p. 150-169.

Schwartzlose, R. A., and J. L. Reid, 1972, Nearshore circulation in the California current: Cal COFI 16, p. 57-65.

Schwartzlose, R. A., 1963, Nearshore currents of the western United States and Baja California as measured by drift bottles: Cal COFI 9, p. 15-22.

Silverman, S. R., 1964, Investigations of petroleum origin and mechanisms by carbon isotope studies, in H. Craig, S. L. Miller and G. L. Wasserberg, eds., Isotope and Cosmic Chemistry: Amsterdam, North-Holland Pub., p. 92-102.

Silverman, S. R., and S. Epstein, 1958, Carbon isotopic compositions of petroleums and other sedimentary organic materials: Am. Assoc. Petroleum Geologists Bull., v. 42, p. 998-1012.

Simons, E. L., 1962, Dissociation pressures of oxides, hydrides, and nitrides, in S. Dushman and J. Lafferty, eds., Scientific foundations of vacuum technique: New York, John Wiley and Sons, p. 738-775.

Smith, C. L., and W. G. MacIntyre, 1971, Initial aging of fuel oil films on sea water: Proc. Joint Conf. on Prev. and Cont. of Oil Spills, Am. Petroleum Inst., p. 457-461.

Stevenson, R. E., R. B. Tibby, and D. S. Gorsline, 1956, The oceanography of Santa Monica Bay, California: Allan Hancock Foundation to Hyperion Engineering, 268 p.

Straughan D., and B. C. Abbott, 1971, The Santa Barbara oil spill: Ecological changes and natural oil leaks: in P. Hepple, ed., Water Pollution by Oil, London Inst. of Petroleum, p. 257-262.

Sweeney, R. E., 1977, Isotopic alteration during Sulfurization of crude oils: 17 p. (unpublished).

Thode, H. G., and J. Monster, 1970, Sulfur isotope abundances and genetic relations of oil accumulations in Middle East basin: Am. Assoc. Petroleum Geologists Bull., v. 54, p. 627-637.

Vredenberg, L. D., and E. S. Cheney, 1971, Sulfur and carbon isotopic investigation of petroleum, Wind River Basin, Wyoming: Am. Assoc. Petroleum Geologists Bull., v. 55, p. 1954-1975.

Wilkinson, E. R., 1971, California offshore oil and gas seeps: California Div. Oil and Gas, v. 57, p. 5-27.

Wilson, R. D., P. Monaghan, A. Osanik, T. Price, and M. Rogers, 1973, Estimate of annual input of petroleum to the marine environment from natural marine seepage: Trans. 23rd Conv. of Gulf Coast Assoc. of Geologists Soc., Houston, Texas, p. 182-193.

Witherspoon, P. A. and R. S. Winniford, 1967, The asphaltic components of petroleum, in B. Nagy and N. Colombo, eds., Fundamental Aspects of Petroleum Geochemistry: New York, Elsevier Pub. Co., p. 261-298.

Yen, T. F., 1974, Structure of Petroleum asphaltene and its significance: Energy Sources, v. 1, p. 447-463.

APPENDICES

APPENDIX A

LABORATORY PROCEDURES

Asphaltene Preparation

The asphaltene fraction was separated from the total oil by using a modified pentane precipitation technique as described by Sachanen (1945). During initial preparations, the extraction and precipitation steps were performed twice to insure complete purification of the asphaltenes. Table A-1 compares the %S, $\delta^{13}C$, and $\delta^{34}S$ for a petroleum sample on which the purification procedure was performed once and twice. The close agreement of the values allowed the discontinuing of repetitive extractions.

The solvent used for initial dissolution of the petroleum or tar sample was benzene, due to the relative ease at which it was separated from the asphaltenes by freeze drying. Due to its extreme carcinogenic nature, benzene was replaced by toluene. This substitution of solvent had no effect on the measured parameters as shown in Table A-2.

The step-by-step preparation procedure is given in Table A-3. A flow diagram of this procedure may be found in O'Neil (1978).

Total Sulfur Determination

Sulfur was determined gravimetrically as barium sulfate prepared by a modified Parr bomb method (Parr Instrument Manual, 1964), outlined

Table A-1. Comparison of measured parameters in the asphaltene fraction of petroleum for single extraction and repetitive extractions.

Sample	$\delta^{13}C$(‰)	$\delta^{34}S$(‰)	%S	%N
Standard #1 Single Extraction	-21.9	+10.7	6.66	1.62
Standard #1 Repetitive	-22.3	+10.1	6.72	1.62
Standard #1 Repetitive	-22.2	+10.2	6.18	--

Table A-2. Comparison of measured parameters in the asphaltene fraction of petroleum with different solvents.

Sample	Solvent	$\delta^{13}C$(‰)	$\delta^{34}S$(‰)	%S
Torrance 9-20-76	Toluene	-23.21	+15.41	7.48
	Benzene	-23.29	+15.63	7.57
Venice 8-26-76	Toluene	-23.02	+ 8.59	7.10
	Benzene	-22.97	+ 8.83	6.57

Table A-3. Asphaltene Preparation Procedure

1. Weigh out sample into soxhlet thimble - record.
2. Place into extraction flask (soxhlet).
3. Measure 500 ml. of toluene into round bottom flask.
4. Hook extraction flask to round bottom flask - turn on variac.
5. After reflux turns clear, remove soxhlet thimble.
6. Weigh thimble and sand - record.
7. Continue distilling of sample - pour excess toluene away until 50 ml. of bottoms remains in flask.
8. Pour 1000 ml. of pentane into 2000 ml. beaker.
9. Insert magnetic stirrer - place on stirrer.
10. Slowly pour bottoms from step 7 into pentane.
11. Cover with saran wrap - allow to stir overnight.
12. Centrifuge and discard supernatant - allow precipitate (asphaltenes) to dry in hood until easy to remove.
13. Transfer to new soxhlet thimble.
14. Set up soxhlet apparatus as in steps 2-5 except use pentane instead of toluene.
15. When reflux turns clear, remove round bottom flask and replace with flask of toluene.
16. Allow to extract until reflux turns clear.
17. Evaporate toluene as in step 7.
18. Remove final solvent by freeze-drying or evaporation.
19. Weigh asphaltenes - record.
20. Calculate percent asphaltene of sample.

in Table A-4. The analytical precision was determined by repetitive analyses to be ±5% of the measurement (Table A-5).

Initial sulfur determinations were contaminated by precipitation of the methyl orange indicator. This problem was eliminated by substitution of distilled water for the indicator during washing of the bomb and periodic checking for complete sulfur removal with only a few milliliters of indicator. Typically, 250 milliliters of wash solution removed all sulfur from the bomb and crucible.

Asphaltene as CO_2 for $\delta^{13}C$ Analysis

The combustion of the asphaltene sample to CO_2 gas was accomplished in an ultra-high vacuum, glass extraction system (Figure A-1). Samples were combusted for 7 minutes in 700mm of oxygen at 900°C and the product gases drawn through the system by opening to vacuum downstream through stopcock K. Long times were required for complete evacuation of the product gases, sometimes requiring 45 to 60 minutes. A new procedure was adopted which flushed the product gases through the system using two volumes of oxygen (approximately 25 scc per volume). This procedure gave identical results to the previous extraction method (Table A-6) yet cut analysis time by two-thirds.

After combustion, the product gases consist of the oxides of C, S, and N, as well as H_2O and excess O_2. The oxides of carbon are oxidized to their highest state as CO_2 by CuO and platinum metal heated to 550°C by the reaction: $CO(g) + 2CuO(s) \rightleftharpoons CO_2(g) + Cu_2O(s)$.

Although CuO is stable at room temperature, at high temperature the compound degasses. A pressure in the vacuum system of 8 to 15

Table A-4. Sulfate Preparation Procedure

---

1. Completely powder asphaltene.

2. Weigh out 0.25 grams of sample into metal crucible.

3. Assemble Parr bomb as follows:
   a. Cover bottom of bomb with distilled water (7 ml).
   b. Attach fuse wire to top. Put crucible in cradle and top into bottom.
   c. Screw on collar.

4. Pump 31 atmospheres oxygen into bomb.

5. Immerse bomb completely in water.

6. Ignite bomb - allow to stand for 3-5 minutes.

7. Release gases slowly.

8. Ready 15 mls of saturated brominated water.

9. Open Parr bomb and pipette about 3 mls of the bromine water into bomb.

10. Thoroughly wash the entire inside of the Parr bomb, top, and crucible with distilled water, collecting the washings in a 400 ml beaker and checking for sulfur with methyl orange indicator (approx. 250 mls of washing).

11. Add the rest of the brominated water, and set on hot plate to simmer to 125 mls.

12. Filter solution, using Whatman #42 filter paper, dry, and weigh unburned sample. The unburned residue should be less than 1% of the original sample.

13. Heat filtrate to a slow boil and add 6 drops conc. HCl.

14. Add 10 mls $BaCl_2$ a few drops at a time to ppt. $BaSO_4$. Stir continuously, continue stirring 2 min after addition of $BaCl_2$.

15. Heat for 1 hr. with watch glass over beaker.

16. Allow to sit overnight.

17. Filter with Whatman #42 paper.

18. Discard filtrate, dry and weigh ppt.

Table A-4. (Con't.)

19. Place ppt. and filter paper into porcelin crucible.

20. Put crucible in cold oven and heat to 1000°C.

21. Weigh ppt. after cooling.

22. Calculate % sulfur and store $BaSO_4$.

Table A-5. Analytical precision of total sulfur content procedure.

Standard #1	Date Run	%S	
	2-28-77	6.35	
	3-01-77	6.10	
	3-06-77	6.00	
	3-24-77	6.65	$\bar{x}$ = 6.41
	3-24-77	6.45	s = 0.34
	3-24-77	6.90	%E = 5.2
Torrance 9-04-76	4-12-77	7.46	
	4-14-77	7.75	
	4-14-77	8.06	
	4-14-77	7.72	
	4-21-77	7.35	
	4-21-77	7.97	
	4-21-77	7.46	
	4-21-77	7.65	
	6-06-77	8.37	$\bar{x}$ = 7.83
	6-06-77	8.19	s = 0.32
	5-23-77	8.01	%E = 4.4
	5-23-77	7.97	

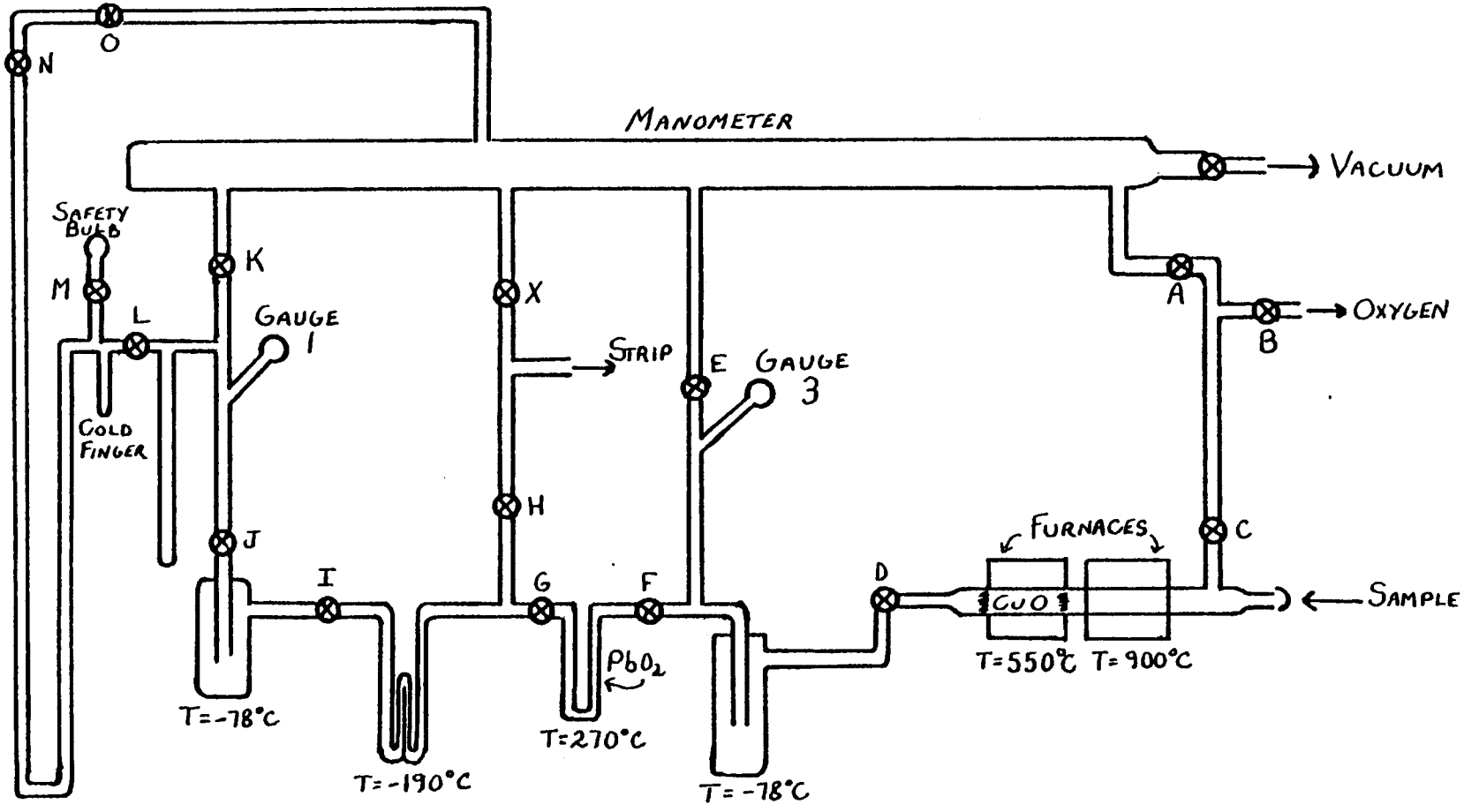

Figure A-1. Ultra-high vacuum glass extraction system for preparation of carbon dioxide gas for isotopic analysis.

microns was not unusual after this compound reached temperature. The reaction for this degassing is:

$$2CuO(s) \rightleftharpoons Cu_2O + \tfrac{1}{2}O_2(g)$$

In addition, the Cu_2O may decompose:

$$Cu_2O(s) \rightleftharpoons 2Cu(s) + \tfrac{1}{2}O_2(g)$$

For these reactions, the equilibrium pressure of oxygen at any temperature may be calculated by:

$$\Delta G = -RT \ln K \qquad \text{Where } K = P^{\frac{1}{2}}_{O_2}$$

$$\Delta G_t = -RT \ln \left(P^{\frac{1}{2}}_{O_2}\right)$$

Rearranging:

$$\log PO_2 = \frac{2\Delta G_t}{4.575\ T} \qquad (P_{O_2} \text{ in atmospheres})$$

or:

$$\log PO_2 = 2.881 + \frac{2\Delta G_t}{4.575\ T} \qquad (P_{O_2} \text{ in mm})$$

The equilibrium pressures for these reactions have been calculated by Simons (1962) and are summarized for the temperature range of interest in Table A-7. It is evident from the calculated pressures that the degassing effect of the CuO will increase as the temperature increases. The degassing does not add contamination to the sample, since the product gas is oxygen.

The oxidized combustion gases are passed through a series of purification traps, designed to separate the CO_2 from the mixture. Water is first removed by passing the gases through a dry ice-isopropyl alcohol bath (-78°C). Oxides of nitrogen and sulfur are removed by heated PbO_2 on quartz wool (270°C) by the reactions:

Table A-6. Evacuation vs. oxygen flush method for preparation of CO_2 from asphaltene.

Sample	$\delta^{13}C$ (evac.) (‰)	$\delta^{13}C$ (flush) (‰)
Torrance 9-04-76	-22.88	-22.77
Venice 9-20-76	-26.24	-26.07
Venice 10-01-76	-26.31	-26.16

Table A-7. Equilibrium oxygen variation with temperature for the reaction: $CuO(s) \rightleftharpoons Cu_2O(s) + \frac{1}{2}O_2(g)$ After Simons (1962).

Temperature (^{o}K)	PO_2 (μ)
800	1.93×10^{-2}
900	1.97
1000	80
1100	1.81×10^{3}

$$NO + PbO_2 \rightleftharpoons PbNO_3$$

$$NO_2 + PbO_2 \rightleftharpoons PbNO_3 + \tfrac{1}{2}O_2$$

$$SO_2 + PbO_2 \rightleftharpoons PbSO_4$$

$$SO_3 + PbO_2 \rightleftharpoons PbSO_4 + \tfrac{1}{2}O_2$$

Although the temperature may vary slightly, it is essential to operate this trap at temperatures lower than 320°C; the decomposition temperature of PbO_2. This trap must be changed when the PbO_2 has been completely converted to sulfur and nitrogen oxides, apparent by the color change from red (PbO_2) to yellow-orange ($PbSO_4$, $PbNO_3$). The remaining CO_2 and any traces of H_2O are trapped at liquid nitrogen temperature (-190°C) in a multi-loop trap. The trapping efficiency was determined during early combustions, as shown in Table A-8.

Assuming an analytical precision of 0.15‰, the fractionation between the CO_2 trapped and CO_2 lost necessary to cause an appreciable error may be calculated as:

$$(\delta_1 - 0.15) = .9725\,\delta_1 + .0275\,\delta_2$$

$$\text{Rearranging: } 0.15‰ = .0275\,\delta_1 - .0275\,\delta_2$$

$$\text{And: } (\delta_1 - \delta_2) = 0.15/.0275 = 5.45‰$$

Table A-9 shows the fractionation of two successive trappings to be 0.05‰; two orders of magnitude less than the required amount.

The analytical precision of the isotopic analysis after extraction and mass spectrometric analysis is shown in Table A-10. Table A-11 gives a summary of the operational procedure.

Table A-8. Trapping efficiency of CO_2 in liquid nitrogen cold bath.

Sample	Expanded Pressure (microns) Trap #1	Trap #2
Torrance 9-04-76	400	8
Torrance 9-04-76	400	11

Trapping efficiency = E = 11/400 = 0.975(100) = 97.5%

Table A-9. Fractionation effect between first and second cold traps for CO_2.

Sample	$\delta^{13}C$(‰) Trap #1	Trap #2
Torrance 9-04-76	-22.09	-22.13
Platform crude CR-23	-22.60	-22.54

Table 10. Replicate analysis of carbon isotope number for determination of analytical precision.

Seep Oil-Coal Oil Point

Run #	$\delta^{13}C$(‰)	Extract. Date	Mass Spec. Date
25	-22.94	3-31-77	4-14-77
26	-23.05	4-12-77	4-14-77
27	-23.04	4-12-77	4-14-77
28	-23.04	4-12-77	5-03-77
29	-23.19	4-13-77	4-14-77
30	-22.97	4-13-77	6-07-77
164	-23.04	8-09-77	8-09-77
167	-22.92	8-11-77	8-12-77

$\bar{x}$ = -23.02

s = .080

Table A-11. Organic Carbon as CO_2 - Preparation Procedure

A. Start Up
1. Turn on furnace 1, furnace 2, and PbO_2 furnace.
2. Set dry ice - isopropyl alcohol baths on traps 1 and 3.
3. Wait for furnaces to reach temperatures:
   furnace 1 - 900°C
   furnace 2 - 550°C
   PbO_2 - 270°C
4. Turn on diffusion pump.

B. Combustion Procedures
1. Weigh out ≃7mg (.007g) of sample and place in a porcelin boat.
2. Close D and A. Feed air into furnace by opening B until pressure = 1 atm.
3. Place boat and magnetic pusher into furnace tube. Close tube.
4. Evacuate tube slowly by closing B and slowly opening A.
5. When P#3 < 100, open D.
6. When P#3 < 20, close D and A.
7. Feed oxygen into furnace tube by opening B. Fill to 700mm. Close C and B.
8. Wait 3 minutes, then open C and A.
9. When P#3 < 100, open D.
10. When P#3 < 20, close D and A.
11. Charge furnace with oxygen as in step B-7.
12. Move sample into furnace.
13. After 5 minutes, close E and G.
14. Open D, read P#3 and record.
15. Place liquid N_2 bath on trap 2.
16. Three minutes after opening D, close H and L. Open G.
17. Open C, release about 1/2 total volume of O_2 (read mercury column). Close C, evacuate for 1 minute.
18. Repeat step 17.
19. Evacuate until P#3 = 300. Close D.
20. Continue evacuation until P#3 = 100. Open H, E, and L.
21. When P#1 = 1, close G, H, and K.
22. Remove liquid nitrogen, warm trap, and record P#1.
23. Freeze CO_2 into cold finger with liquid N_2.
24. Open K, close L.
25. Warm up cold finger - read manometer height and record.
26. Close K and J. Open L.
27. Trap CO_2 into sample tube using liquid nitrogen.
28. Pull off sample using torch - label.
29. Return to step B-1.

C. Shut Down
1. Reverse Start-Up steps.

Barium Sulfate as Sulfur Dioxide for $\delta^{34}S$ Analysis

Barium sulfate was combusted to SO_2 by a direct torching method (Bailey & Smith, 1972) in an ultra-high vacuum, glass extraction system (Figure A-2). In the presence of excess oxygen, sulfur trioxide may be formed by the reaction:

$$BaSO_4 \rightleftharpoons BaO + SO_3$$

The sulfur trioxide may then dissociate:

$$SO_3 \rightleftharpoons SO_2 + \tfrac{1}{2}O_2$$

The effect of SO_3 formation is a fractionation of the sulfur isotopes between the two oxides; the more oxidized species being enriched in the heavier isotope (Sakai, 1957).

Prevention of SO_3 formation may be accomplished by two methods:

(1) Keeping the PO_2 below a critical value during combustion of the Barium sulfate.

(2) Incorporating a heated metallic copper trap (800°C) into the extraction system to reduce the PO_2.

Both techniques were employed in this laboratory. In Table A-12, the $\delta^{34}S$ values for samples run under various conditions are listed.

Examination of this table indicates that runs #6, #2, and #2a are significantly lower than the other analyses of the same sample. In each case, the sample was combusted with the copper furnace off and no control on the maximum oxygen pressure. In addition, analyses performed with the furnace off agreed with analyses with the furnace on, so long as the oxygen pressure during combustion was kept below 200 microns.

The standard deviation of the analyses for each sample is

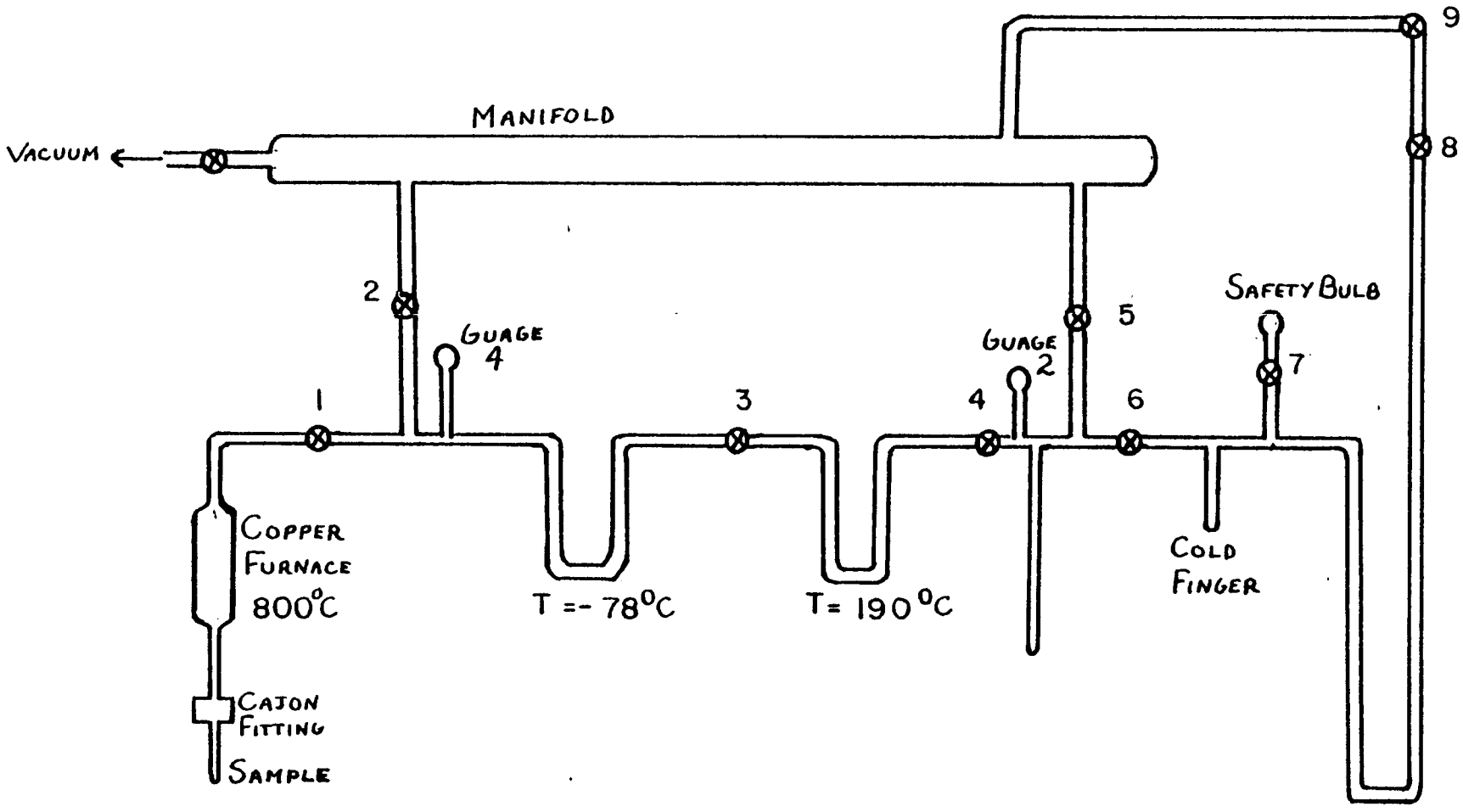

Figure A-2. Ultra-high vacuum glass extraction system for preparation of sulfur dioxide gas for isotopic analysis.

Table A-12. Sulfur isotope ratio for repetitive analysis of two samples under different operating conditions.

Standard #1 8-26-76

Run #	$\delta^{34}S$ (‰)	Operating Conditions
1	+ 9.60	Furnace off, PO_2 = 500
6	+ 8.19	Furnace off, PO_2 = 1000
2	+ 8.86	Furnace off, direct trapping
2a	+ 8.96	Furnace off, PO_2 = 190
5	+ 9.49	Furnace on, PO_2 = 190
12	+ 9.30	Furnace on, PO_2 = 190
14	+ 9.32	Furnace on, PO_2 = 190
134	+10.40	Furnace on, PO_2 = 190

$\bar{x}$ = 9.62 (neglecting runs 6, 2, 2a)

s = .45

Torrance 9-04-76

9	+12.66	Furnace off, PO_2 = 200
15	+12.34	Furnace on, PO_2 = 200
21	+12.46	Furnace on, PO_2 = 180
22	+12.42	Furnace on, PO_2 = 180
146	+12.00	Furnace on, PO_2 = 190

$\bar{x}$ = 12.38

s = .24

indicated. An average precision for these analyses may be taken as ±.35‰. Analytical error may have been introduced by several means:

(1) Formation of SO_3 during combustion.

(2) Incorrect temperature of iso-hexane trap (too high or low).

(3) Mass spectrometric analysis.

After the samples were fully combusted, the product gases (SO_2, H_2O, CO_2) were passed through a series of cold traps. Water was removed by a dry ice-isopropyl alcohol cold trap (-78°C). The SO_2 and small amounts of CO_2 present were trapped in a liquid nitrogen bath (-190°C) and separated from one another by warming to -125°C using a liquid nitrogen-isohexane bath. SO_2 remained in the trap while CO_2 was evacuated. The SO_2 was measured for volume manometrically and collected for isotopic analysis.

The operational procedure is summarized in Table A-13.

Table A-13. Barium Sulfate as SO_2 - Preparation Procedure.

A. Line Preparation
   1. Turn on diffusion pump.
   2. Turn on Cu furnace (variac 72v) and let it heat up for ½ hr.
   3. Mix isopropyl alcohol and dry ice until pasty in a long thermos. This is trap (a).
   4. Pour liquid nitrogen into long thermos, this is trap (b).
   5. Prepare iso-hexane trap by slowly adding liquid N_2 to iso-hexane until temperature is $-125^{o}C$, trap (c).

B. Sample Preparation
   1. Weigh out 30mg of $BaSO_4$ sample.
   2. Transfer to sample tube.
   3. Add approximately the same amount of quartz powder to tube.
   4. Plug the tube with a small amount of quartz wool.

C. Sample Run
   1. Connect sample tube to line just below Cu furnace.
   2. Evacuate entire line through valves 2 & 5 until P#4 < 4.
   3. Close valves 2 & 6. Put traps (a) & (b) on.
   4. Burn for 7 minutes or until P#4 stays at less than 10, making certain that P#4 is never greater than 200 microns.
   5. Let line evacuate until P#4 < 4.
   6. Close valves 3 & 5, open 6 before closing 5. Take trap (b) off & let the gas warm up. Read P#2.
   7. Open valve 6 and freeze gas into cool finger with N_2 until P#2 < 5. Record pressure.
   8. Close valve 4.
   9. Replace N_2 quickly with trap (c) and wait until P#2 is stable. Read CO_2 pressure from P#2.
   10. Evacuate CO_2 through valve 5 until P#2 < 5.
   11. Close valves 5 & 6. Remove trap (c) and let cold finger warm up.
   12. Read manometer
   13. Open valve 6 and let gas into torch tube.
   14. Freeze gas in torch tube with N_2 until P#2 < 5.
   15. Torch off sample.

APPENDIX B

EQUIPMENT CALIBRATION

Manometers

Sample volumes on both the CO_2 and SO_2 vacuum extraction systems were measured by a mercury manometer. Calibrations were performed by using a known volume of CO_2 gas at a measured temperature and pressure.

Combining Boyles and Charles laws: $\frac{V_1 P_1}{T_1} = \frac{V_2 P_2}{T_2}$

Where: V_1 = known volume (cc)

P_1 = measured gas pressure (mm)

T_1 = room temperature (^{o}C)

P_2 = standard pressure (mm)

T_2 = standard temperature (^{o}C)

V_2 = volume of gas in scc

The calibration data for the carbon and sulfur extraction system manometers are given in Table A-14.

The manometer is typically read as millimeters of mercury during analysis, thus a plot of manometer reading vs. volume (scc) is useful. Ignoring temperature effects (since small):

$$V_1 P_1 = V_2 P_2$$

But: $V_2 = V_0 + \Delta V$ See Figure A-3

And: $\Delta V = A \Delta h$

Table A-14. Carbon and Sulfur Extraction Line Manometer Calibration Data.

(A) Carbon Line

Bulb	V_1 (cc)	P_1 (mm)	Manometer Reading	P_2 (mm)	V_2 (scc)
Open	37.09	96.30	92.30	39.75	43.24
Open	37.09	18.20	69.55	10.10	8.19
Closed	37.09	18.20	106.50	78.80	8.19
Open	37.09	21.95	70.60	12.10	9.92
Closed	37.09	21.95	113.45	98.90	9.92
Open	37.09	46.8	77.80	25.40	21.14
Open	37.09	8.6	66.70	4.80	3.89
Closed	37.09	1.5	68.70	8.50	0.68
Open	37.09	1.5	64.60	0.90	0.68
Closed	37.09	15.45	98.90	64.65	6.98
Open	37.09	15.45	68.50	8.15	6.98
Closed	37.09	3.2	71.50	13.75	1.45
Closed	37.09	6.60	81.30	32.15	2.98
Open	37.09	6.60	66.30	4.0	2.98
Closed	37.09	1.25	67.85	6.90	1.25
Open	37.09	1.25	64.50	0.7	1.25
Closed	6.93	114.50	112.5	90.1	9.67
Closed	6.93	7.40	68.2	7.6	.62
Closed	6.93	0.6	64.5	0.8	.05
Closed	6.93	118.2	114.15	93.20	10.00
Closed	6.93	7.80	68.50	8.20	0.66
Closed	6.93	0.50	64.50	0.70	0.04
Closed	6.93	33.2	81.30	32.1	2.80
Closed	6.93	108.6	111.60	88.5	7.15
Closed	6.93	7.50	68.50	8.2	0.63
Closed	6.93	0.50	64.50	1.3	0.04
Closed	6.93	74.9	96.9	61.3	6.34
Closed	6.93	111.2	111.12	87.9	9.41
Closed	6.93	37.5	81.4	32.4	3.17
Closed	6.93	82.1	100.5	65.5	6.95
Closed	6.93	19.5	74.0	18.5	1.65
Closed	6.93	6.3	67.2	5.9	0.53
Closed	6.93	122.5	116.2	97.2	10.37
Closed	6.93	35.9	80.7	31.1	3.04

Table A-14. (Con't)

(B) Sulfur Line

V_1 (cc)	P_1 (mm)	Manometer Reading	V_2 (scc)
37.09	56.7	118.1	27.7
37.09	16.0	83.0	7.8
37.09	14.3	80.5	7.0
37.09	4.1	68.4	2.0
37.09	8.2	74.0	4.0
37.09	3.2	66.4	1.6
37.09	56.5	116.8	27.6
37.09	44.2	108.5	21.6
37.09	11.7	78.1	5.7
37.09	7.0	72.3	3.4
37.09	2.0	65.9	1.0
37.09	44.7	108.6	21.9
37.09	28.5	94.9	13.9
37.09	33.5	98.5	16.3
37.09	23.2	89.9	11.3
37.09	37.7	103.1	18.4
37.09	51.2	113.8	25.0
37.09	14.4	80.9	7.0
37.09	57.1	118.0	27.9

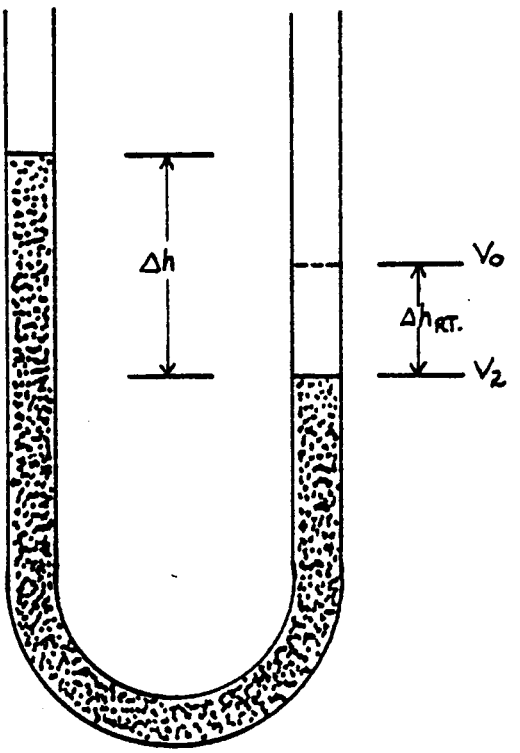

Figure A-3. Parameters used in derivation of volume dependence with height for a standard mercury manometer.

Thus: $P_1V_1 = P_2 (V_0 + A\Delta h)$

But: $P_2 = \Delta h = 2\Delta h$ (right) See Figure 3

Hence: $P_1V_1 = (\Delta hV_0 + \frac{1}{2}A\Delta h^2)$

A graph of the measured volume vs Δh should be nearly linear for low volumes, but becomes non-linear as V_1 increases.

Both extraction systems contain a large volume (50 cc) saftey bulb to be used in case of excessive gas pressure. Carbon line manometer calibrations were performed with the safety bulb on-line and off-line (Table A-14). Sulfur line calibrations were performed only with the bulb off-line. The calibration data is shown graphically in Figures A-4 and A-5.

Vacuum Gauges

Vacuum was measured in the extraction systems by Televac thermocouple gauges (Fredericsk Company) connected to a panel meter ($\pm$2% precision). Calibrations of thermocouple and meter were performed initially by the manufacturer and repeated periodically in the laboratory.

The laboratory calibration consisted of cross-calibration with a known high vacuum source. Calibration data is given in Table A-15. Gauges #2, #3, and #4 were adjusted to agree with #1 after each test. It is recommended that this calibration be performed every few months during operating of the extraction systems.

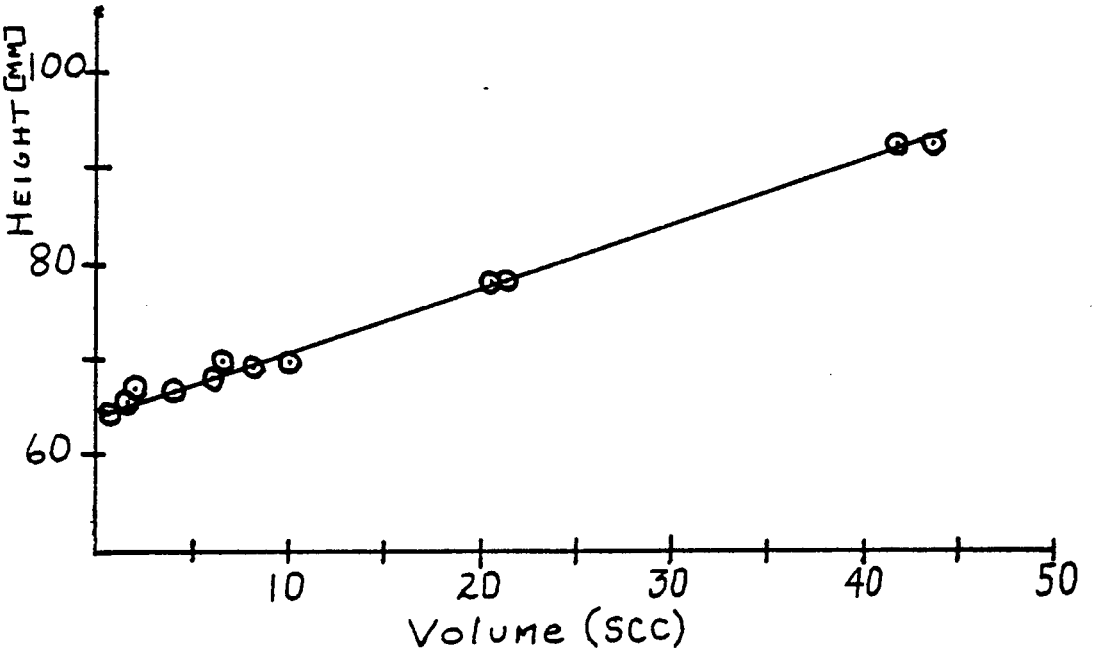

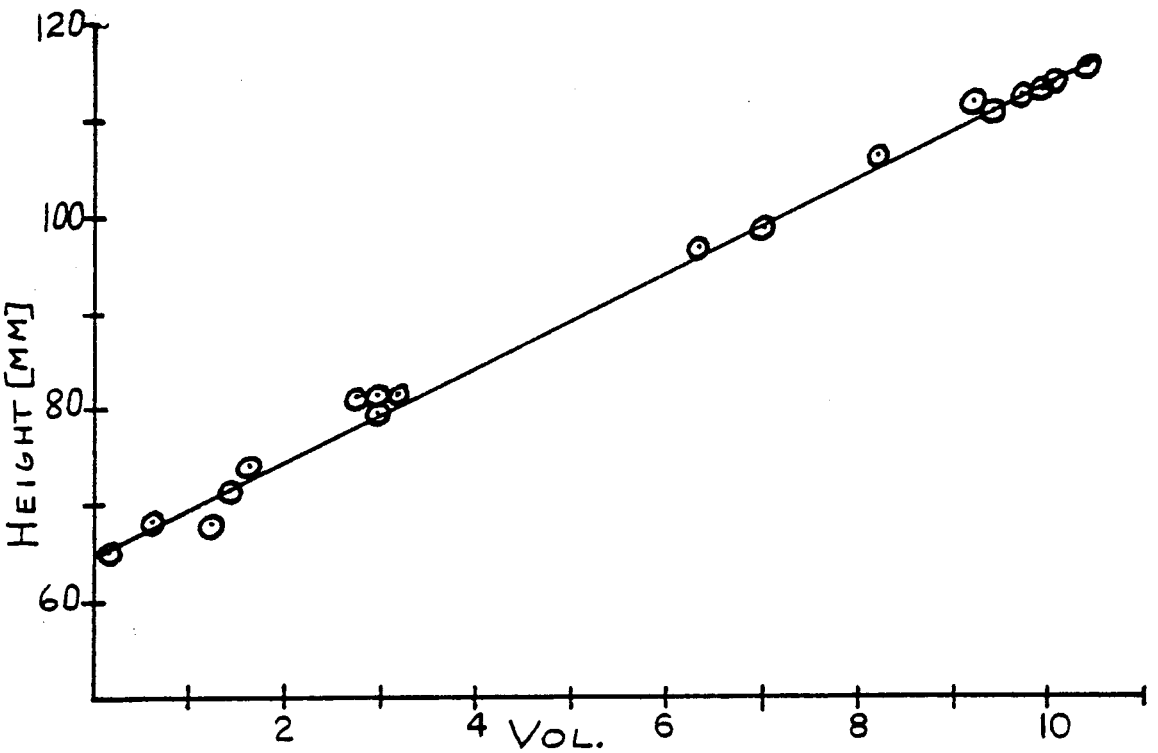

Figure A-4. Calibration data for mercury manometer on the carbon isotope extraction system.

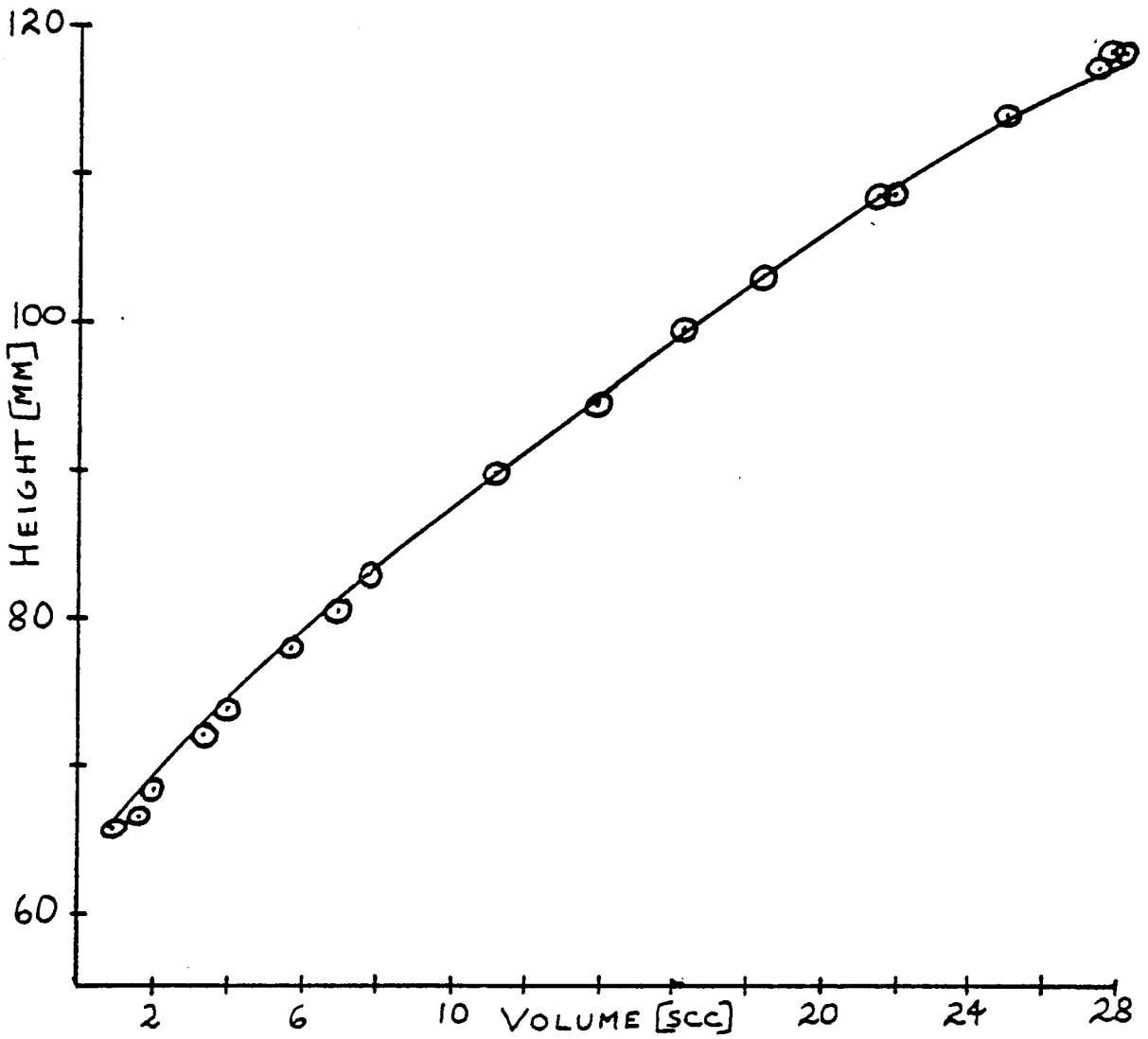

Figure A-5. Calibration data for mercury manometer on the sulfur isotope extraction system.

Table A-15. Calibration data for Televac thermocouple gauges. (Laboratory calibration data only).

Connected to known vacuum source:

Date	Known Vacuum (Microns)	Gauge # #1	#3
1-26-77	0-1	0.5	6.5
1-27-77	0-1	0.5	6.5

Connected to CO_2 and SO_2 extraction systems:

Date	Gauge # #1	#2	#3	#4
3-12-77	1.0	15.5	3.5	10.5
6-06-77	0.9	2.5	2.2	2.5

APPENDIX C

DATA CORRECTIONS

Instrument Fluctuation Corrections

A shift in the $\delta^{34}S$ values for samples analyzed on the mass spectrometer after November, 1977 became evident upon comparison with repetitive samples analyzed before this date (Table A-16). A check on this shift was performed by comparing measured values of standard samples analyzed before and after November, 1977 (Table A-17).

Based upon known values of $\delta^{34}S$ for seep oils from prior studies, it was determined that the analyses prior to November, 1977 were isotopically light.

Hence, the $\delta^{34}S$ values for all samples analyzed before November, 1977 were corrected by addition of +2.30‰. This constant was determined by taking a mean of the apparent shift of the repetitive samples (Table A-18).

The reason for this shift in values is unknown. The most likely cause is probably an incorrect determination of the mass spectrometer working standard used during runs prior to November, 1977.

Tank Oxygen Corrections

The basic measurement performed by a mass spectrometer is the relative abundance of the isotopes of a given element of interest from

Table A-16. $\delta^{34}S$ of repetitive samples analyzed on mass spectrometer before and after November, 1977.

Sample	Run #	Date Extracted	Date Analyzed	$\delta^{34}S$(‰)
S-2B 9-17-76	97	9-25-77	11-15-77	+11.59
	28	6-21-77	12-16-77	+13.99
S-3A 10-16-76	47	9-08-77	11-15-77	+10.52
	114	11-27-77	12-16-77	+12.64
PW #1	36	8-31-77	11-15-77	+ 5.93
	113	11-27-77	12-16-77	+ 7.76
S-5 11-5-76	27	6-21-77	11-15-77	+10.03
	111	11-27-77	12-16-77	+12.20

Table A-17. $\delta^{34}S$ for two standards, analyzed on mass spectrometer before and after November, 1977.

Sample	Run #	Date Extracted	Date Analyzed	^{34}S(‰)
Stan #1	1	3-11-77	11-01-77	+ 9.60
	5	4-04-77	11-01-77	+ 9.49
	12	5-17-77	11-01-77	+ 9.30
	14	5-24-77	11-01-77	+ 9.32
	134	12-20-77	2-13-78	+12.81
$1\text{-}B_2$ 9-4-76	9	5-10-77	11-01-77	+12.66
	15	5-24-77	11-01-77	+12.34
	21	6-07-77	11-01-77	+12.46
	22	6-07-77	11-01-77	+12.42
	146	1-13-78	1-26-78	+14.39

Table A-18. Shift in $\delta^{34}S$ of repetitive samples analyzed before and after November, 1977.

Sample	$\Delta\delta^{34}S$
S-2B 9-17-76	-2.40
S-3A 10-16-76	-2.21
PW #1	-1.83
S-5 11-5-76	-2.17
Stan #1	-3.38
$1\text{-}B_2$ 9-04-76	-1.92
$\bar{x}$ =	-2.30

a sample gas. Generally, the isotopic ratio of the element is not measured directly. For example, the isotopic ratio of carbon ($^{13}C/^{12}C$) is measured from carbon dioxide gas by simultaneously collecting masses 45 and 46. The ratio is given by:

$$R_{45} = \frac{^{13}C\ ^{16}O\ ^{16}O + {}^{12}C\ ^{16}O\ ^{17}O}{^{12}C\ ^{16}O\ ^{16}O}$$

Similarly, the isotopic ratio of sulfur ($^{34}S/^{32}S$) is measured from sulfur dioxide gas as a ratio of masses 66 to 64. The ratio is given by:

$$R_{66} = \frac{^{34}S\ ^{16}O\ ^{16}O + {}^{32}S\ ^{16}O\ ^{18}O}{^{32}S\ ^{16}O\ ^{16}O}$$

In the calculation of absolute isotopic ratios relative to national standards, a correction must be made for the ^{17}O and ^{18}O contributions to the 45 and 66 mass peaks, respectively.

Craig (1957) studied the oxygen isotope composition of carbon dioxide produced by the combustion of carbon and derived an expression for the correction of the carbon isotopic ratio as:

$$\delta^{13}C = \delta(45)\ \frac{R_{45(std)}}{R_{13(std)}} - \frac{R_{17(std)}}{2R_{13(std)}}\ \delta^{18}O$$

Where: $\delta^{13}C$ is the corrected isotopic value,

$\delta(45)$ the measured value,

$\delta^{18}O$ the isotopic ratio of the tank oxygen, and

$R_{45}(std)$, $R_{17}(std)$, $R_{13}(std)$ the measured mass ratios 45/44, 17/16, 13/12 in the standard gas, respectively.

Similarly, Claypool (1974) derived an expression for the correction of sulfur isotope measurements as:

$$\delta^{34}S = \delta(66)\ \ 1 + \frac{R_{18(std)}}{R_{34(std)}} - \frac{R_{18(std)}}{R_{34(std)}}\ \delta^{18}O$$

Where: $\delta^{34}S$ is the corrected isotopic value,

$\delta(66)$ the measured value,

$\delta^{18}O$ the isotopic ratio of the tank oxygen, and

$R_{34}(std)$, $R_{18}(std)$ the measured mass ratios 34/32 and 18/16 in the standard gas, respectively.

Hence, suitable corrections for the carbon and sulfur isotopic ratios of organic constituents may be calculated by measurement of the oxygen isotopic ratio of the tank oxygen.

APPENDIX D

CONTROLLED WEATHERING EXPERIMENT

The controlled weathering of three oils was conducted at the USC Catalina Marine Science Center. System design consisted of 400 liter plexi-glass tanks with constant seawater flow and bottom drain.

The flushing time, τ, is fixed by the flow rate of seawater into and out of the system (assuming steady state).

$$\tau = \frac{\text{Volume of tank}}{\text{Flow rate}} = \frac{(120 \times 76 \times 45)\ \text{cc}}{900\ \text{cc/min}}$$

$$\tau = 410 \text{ min} = 7 \text{ hours}$$

Hence, the tank was completely flushed on the average of 3 times per day.

Weathering of the Sumatra crude and the platform crude was as follows:

Initial set-up:	5-04-77	
Sampling dates:	6-06-77	33 days of weathering,
	6-23-77	50 days of weathering,
	8-12-77	100 days of weathering.

The weathering of seep oil began later:

Initial set-up:	8-12-77	
Sampling dates:	9-23-77	42 days of weathering.

APPENDIX E

SAMPLE CODES

Samples were coded for easy handling and convenience. The code consists of three criteria:

(1) Type of oil or tar sample (seep, platform, beach, tanker, etc.).

(2) Location of sample and aliquot (if multiple samples taken).

(3) Date.

Seep Oils - the general code for seep oils is: $S\text{-}X_{z}^{y}$.

Where: S designates seep,
X seep number,
y aliquot (A,B,C,...),
z date.

Offshore production (platform) crudes - the general code for these samples is: $CR\text{-}X_{z}$.

Where: CR designates a platform crude,
X designates platform number,
z designates date.

Tanker Crudes - the general code is: X_{z}.

Where: X designates number of crude,
z designates date.

Beach Tars - the general code is: $X\text{-}y_{z}$.

Where: X designates beach number,
y designates aliquot,
z designates date.

Table A-16 gives the location of the various oil and tar samples by number.

Table A-19. Locations of analyzed samples by code number.

Sample	Location	Number (x)
Seep Oils	Coal Oil Point	1
	Isla Vista	2
	Goleta	3
	Carpinteria	4
	Redondo Canyon	5
	Manhattan	6
Platform Crudes	Dos Cuadras (offshore) Platform Hillhouse	1
	Huntington Beach PRC 426-4104	3
	Carpinteria #012 Standard Oil Co.	7
	Elwood Field 208 #14	12
	West Montalvo 735.1 C-3	13
	Dos Cuadras (offshore) Platform Hillhouse	22
	Huntington Beach 91 #J-50	23
	Rincon 145 #6	25
	Carpinteria SASC 3133-3150-40001	26
	Rincon PRC 145.1	31
	South Elwood 3120 #3	33
Beach Tars	Torrance	1
	Venice	10
	Topanga North	20
	Seal Beach	30
	Blacks Beach	50
	Coal Oil Point	60
	Morro Bay	100
Tanker Crudes	Sumatra	116048
	Arabia	117328